H. Silm
Clinic of Dermatology, University of Tartu, Estonia

S. Kõks[a,b,c,*]
[a]*Department of Physiology, University of Tartu, Estonia*
[b]*Centre of Translational Medicine, University of Tartu, Estonia*
[c]*Institute of Veterinary Medicine and Animal Sciences, Estonian University of Life Sciences, Estonia*

*Corresponding author at: Department of Physiology, University of Tartu, 19 Ravila Street, 50411 Tartu, Estonia. Tel.: +372 7 374 335; fax: +372 7 374 332
E-mail address: Sulev.Koks@ut.ee (S. Kõks)

27 April 2010

doi:10.1016/j.jdermsci.2010.08.004

Letter to the Editor

ABCA12 dysfunction causes a disorder in glucosylceramide accumulation during keratinocyte differentiation

Harlequin ichthyosis (HI) is an autosomal recessive congenital ichthyoses, and patients of this disease frequently present with severe hyperkeratosis and scales over all of their epidermal surfaces. Recently, the gene encoding ABCA12 was identified as a causative gene for HI [1]. Since dysfunction in ABCA12 causes a decrease in epidermal ceramide (Cer) content concomitantly with loss of the skin lipid barrier, ABCA12 is thought to regulate epidermal generation of Cer. However, so far no direct target of ABCA12 has been identified. Thus, we attempted to study the substrate of ABCA12 by generating an ABCA12-deficient keratinocyte cell line and then comparing its sphingolipid metabolism to that of a normal keratinocyte cell line. Keratinocytes were isolated from a HI patient and a healthy donor [1], then were immortalized by expressing the T-antigen of SV40. After 15 passages, the morphology of the cells became uniform and we confirmed the expression of the SV40 T-antigen by Western blotting (Fig. 1A and B). The cell lines thus generated from the cells isolated from the HI patient and healthy donors were named HIKT and KT1, respectively. Genomic analysis revealed one mutation in the HIKT cells, from A to G adjacent a splice acceptor site of exon 24 (Fig. 1C). This mutation produced two splice variants of 674-bp and 513-pb (Fig. 1D). The 674-bp results from 9-bp lost from exon 24, and the 513-bp results from 170-bp lost from exon 24. This mutation has been reported to seriously affect the function of the ABCA12-protein [1]. We have successfully established an ABCA12-impaired keratinocyte cell line.

Several groups have demonstrated that the expression level of ABCA12 increases during the differentiation of keratinocytes, so that anaplastic keratinocytes express only low levels of ABCA12 [2,3]. As shown in Fig. 2A, anaplastic KT1 scarcely expresses any ABCA12. So, we attempted to induce differentiation of KT1 and HIKT cells, and thereby express high levels of ABCA12 in the cells. We induced differentiation in KT1 and HIKT cells and confirmed the differentiation by measuring the differentiation marker involcurin, which increased significantly in both cell lines during differentiation (3.1-fold increase in KT1 and 2.4-fold increase in HIKT) (Fig. 2A). We further found that ABCA12 also increased during differentiation, with especially high levels of expression at 7 days after induction in the HIKT cells. Following the induction of differentiation in KT1 and HIKT cells, their sphingolipid metabolism was examined at 7 days by labeling the cells with [^{3}H]dihydosphingosine or [^{14}C]galactose (Fig. 2B and C, respectively). Interestingly, apparent accumulations of [^{3}H]GlcCer (Fig. 2B) and [^{14}C]GlcCer (Fig. 2C) were observed in KT1 cells at 7 days post-induction compared to HIKT cells (203% increase at [^{3}H]GlcCer and 181% increase at [^{14}C]GlcCer, respectively). It is noteworthy that [^{14}C]gangliosides levels in KT1 cells were lower rather than equal to levels in HIKT cells (31% reduction), despite the accumulation of GlcCer. Since the ABCA12 is known to localize at lamellar bodies (LBs) in keratinocyte [4], this result indicates that differentiated KT1 cells aggressively accumulate GlcCer in LBs and not in the Golgi apparatus. Our results clearly demonstrate that ABCA12 deficiency impairs the GlcCer accumulation in LBs, thereby strongly indicating that ABCA12 transports GlcCer to the inner leaflet of LBs (Fig. 2D). Mass spectrometer analysis of accumulated

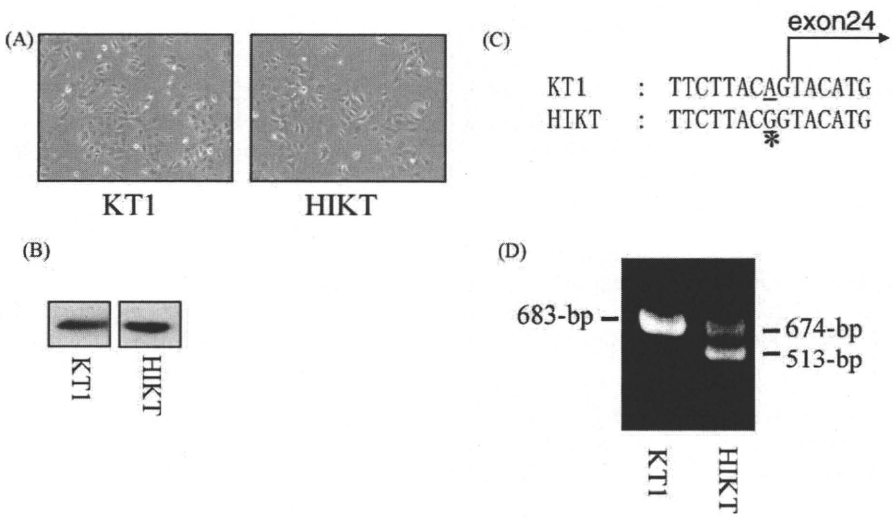

Fig. 1. KT1 and HIKT keratinocyte cell lines. KT1 and HIKT keratinocyte cell lines were generated by introducing the SV40 T-antigen into the cells using the culture supernatant of ΨCRIP-pMFGtsT (distributed from RIKEN cell bank, Tsukuba, Japan). After 15 passages, KT1 and HIKT cells exhibited similar morphology (A), and expected expression levels of T-antigen as examined by Western blotting using anti-SV40 LT (BD biosciences, NJ) (B). Genomic structures of KT1 and HIKT cells neighboring exon 24 (C). *A mutation from A to G in HIKT cells. RT-PCR analysis of mRNA fragments around the exon 23–24 boundary was performed as described previously [1] (D).

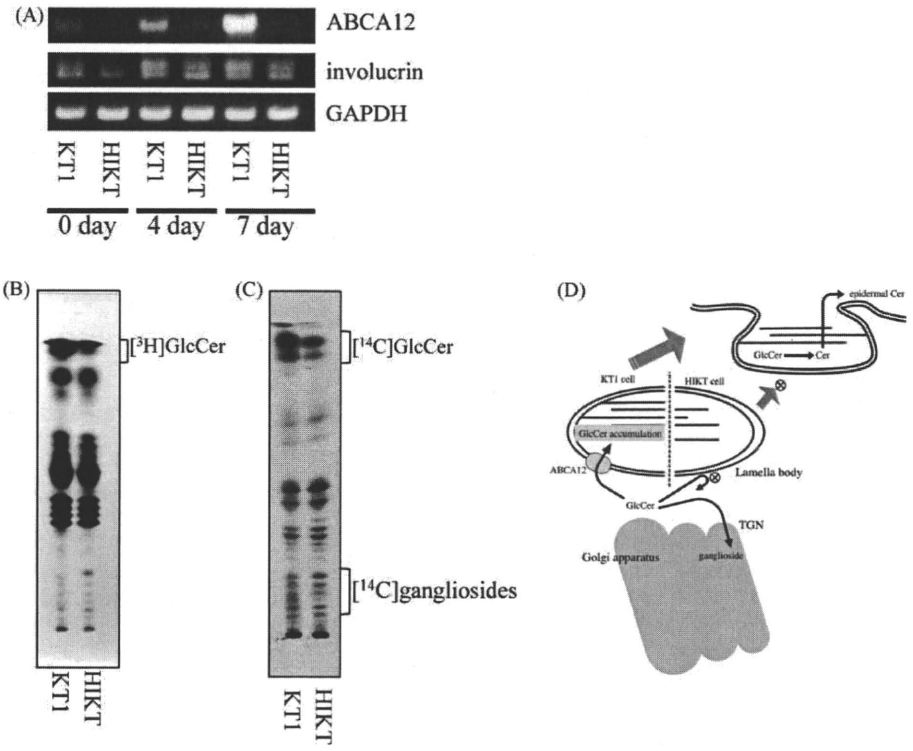

Fig. 2. Sphingolipids in KT1 and HIKT 4 days after induction of differentiation. (A) To induce differentiation, HIKT and KT1 cells were cultured in a DMEM/F-12 (2:1) mixture containing 10% fetal bovine serum, 1.2 mM Ca^{2+}, 10 μg/ml insulin, and 0.4 μg/ml ascorbic acid (differentiation medium) at 39 °C. Before (0 day) and 4 days and 7 days after induction, total RNA was isolated from each cell line, and semi-quantitative RT-PCR was performed using primers for ABCA12, 5′-GAATTGCAAACTGGAAGGAACTCCC-3′ and 5′-GAGTCAGCTAGGATTAGACAGC-3′; for involcurin, 5′-CTCCTCAAGACTGTTCCTCC-3′ and 5′-GCAGTCATGTGCTTTTCCTCTTGC-3′; for GAPDH, 5′-ATCACTGCCACCCAGAAGAC TGTGGA-3′ and 5′-GAGCTTGACAAAGTTGTCATTGAGAGC-3′. Seven days after induction of differentiation, HIKT and KT1 cells (10^6) were metabolically labeled with [^{3}H]dihydrosphingosine (2 μCi) (B) or [^{14}C]galactose (5 μCi) (C), then lipids were extracted and applied to HPTLC plates as described previously [5]. The HPTLC plates were developed with chloroform/methanol/0.05% $CaCl_2$ (60:35:8). The data are representative of tree independent experiments. (D) A possible mechanism of how to generate epidermal ceramides.

GlcCer will provide advanced information about substance preference of ABCA12. This remains for future study.

References

[1] Akiyama M, Sugiyama-Nakagiri Y, Sakai K, McMillan JR, Goto M, Arita K, et al. Mutations in lipid transporter ABCA12 in harlequin ichthyosis and functional recovery by corrective gene transfer. J Clin Invest 2005;115:1777–84.
[2] Jiang YJ, Lu B, Kim P, Paragh G, Schmitz G, Elias PM, et al. PPAR and LXR activators regulate ABCA12 expression in human keratinocytes. J Invest Dermatol 2008;128:104–9.
[3] Jiang YJ, Uchida Y, Lu B, Kim P, Mao C, Akiyama M, et al. Ceramide stimulates ABCA12 expression via peroxisome proliferator-activated receptor {delta} in human keratinocytes. J Biol Chem 2009;284:18942–5.
[4] Yamanaka Y, Akiyama M, Sugiyama-Nakagiri Y, Sakai K, Goto M, McMillan JR, et al. Expression of the keratinocyte lipid transporter ABCA12 in developing and reconstituted human epidermis. Am J Pathol 2007;171:43–52.
[5] Takeda S, Mitsutake S, Tsuji K, Igarashi Y. Apoptosis occurs via the ceramide recycling pathway in human HaCaT keratinocytes. J Biochem 2006;139:255–62.

Susumu Mitsutake[1]
Department of Biomembrane and Biofunctional Chemistry, Faculty of Advanced Life Sciences, Hokkaido University, Nishi 11, Kita 21, Kita-ku, Sapporo 001-0021, Japan

Chihiro Suzuki[1]
Department of Biomembrane and Biofunctional Chemistry, Faculty of Advanced Life Sciences, Hokkaido University, Nishi 11, Kita 21, Kita-ku, Sapporo 001-0021, Japan

Masashi Akiyama
Department of Dermatology, Hokkaido University Graduate School of Medicine, Nishi 7, Kita 15, Kita-ku, Sapporo 060-8638, Japan

Kiyomi Tsuji
Department of Biomembrane and Biofunctional Chemistry, Faculty of Advanced Life Sciences, Hokkaido University, Nishi 11, Kita 21, Kita-ku, Sapporo 001-0021, Japan

Teruki Yanagi, Hiroshi Shimizu
Department of Dermatology, Hokkaido University Graduate School of Medicine, Nishi 7, Kita 15, Kita-ku, Sapporo 060-8638, Japan

Yasuyuki Igarashi*
Department of Biomembrane and Biofunctional Chemistry, Faculty of Advanced Life Sciences, Hokkaido University, Nishi 11, Kita 21, Kita-ku, Sapporo 001-0021, Japan

*Corresponding author at: Hokkaido University, Department of Biomembrane and Biofunctional Chemistry, Graduate School of Pharmaceutical Sciences, Nishi 11, Kita 21, Kita-ku, Sapporo 001-0021, Japan.
Tel.: +81 11 706 9086; fax: +81 11 706 9047
E-mail address: yigarash@pharm.hokudai.ac.jp (Y. Igarashi)

[1]These authors contributed equally to this work.

8 April 2010

doi:10.1016/j.jdermsci.2010.08.012

Human IgG1 Monoclonal Antibody against Human Collagen 17 Noncollagenous 16A Domain Induces Blisters via Complement Activation in Experimental Bullous Pemphigoid Model

Qiang Li,*[,1] Hideyuki Ujiie,*[,1] Akihiko Shibaki,* Gang Wang,* Reine Moriuchi,* Hong-jiang Qiao,* Hiroshi Morioka,[†] Satoru Shinkuma,* Ken Natsuga,* Heather A. Long,* Wataru Nishie,* and Hiroshi Shimizu*

Bullous pemphigoid (BP) is an autoimmune blistering disease caused by IgG autoantibodies targeting the noncollagenous 16A (NC16A) domain of human collagen 17 (hCOL17), which triggers blister formation via complement activation. Previous in vitro analysis demonstrated that IgG1 autoantibodies showed much stronger pathogenic activity than IgG4 autoantibodies; however, the exact pathogenic role of IgG1 autoantibodies has not been fully demonstrated in vivo. We constructed a recombinant IgG1 mAb against hCOL17 NC16A from BP patients. In COL17-humanized mice, this mAb effectively reproduced a BP phenotype that included subepidermal blisters, deposition of IgG1, C1q and C3, neutrophil infiltration, and mast cell degranulation. Subsequently, alanine substitutions at various C1q binding sites were separately introduced to the Fc region of the IgG1 mAb. Among these mutated mAbs, the one that was mutated at the P331 residue completely failed to activate the complement in vitro and drastically lost pathogenic activity in COL17-humanized mice. These findings indicate that P331 is a key residue required for complement activation and that IgG1-dependent complement activation is essential for blister formation in BP. This study is, to our knowledge, the first direct evidence that IgG1 Abs to hCOL17 NC16A can induce blister formation in vivo, and it raises the possibility that IgG1 mAbs with Fc modification may be used to block pathogenic epitopes in autoimmune diseases. *The Journal of Immunology*, **2010, 185: 7746–7755.**

Bullous pemphigoid (BP) is the most common autoimmune subepidermal blistering disease (1, 2). Circulating autoantibodies target human type XVII collagen (human collagen 17 [hCOL17]), also known as BP Ag 2 (BPAG2) or BP180, which is a major component in hemidesmosome-anchoring filament complexes at the epidermal basement membrane zone (BMZ) (3–9). The major pathogenic epitope of BP autoantibodies is present at the extracellular noncollagenous 16A (NC16A) domain, which has distinctive diversity among different species (10–12). Deposition of anti-hCOL17 autoantibodies at the BMZ triggers sequential inflammatory cascades, including complement activation, degranulation of dermal mast cells, infiltration of eosinophils and neutrophils, and subepidermal blister formation elicited by proteinases derived from the inflammatory cells (13–17).

In the inflammatory mechanism of BP, the IgG-dependent classical complement pathway plays an important role in autoimmune blister formation. Complement components including C1q, C3 and C4 are detected at the dermal-epidermal junction (DEJ) in the skins of patients and experimental BP model mice (17–21). BP phenotypes have been abolished by the inhibition of C1q using neutralizing Abs in experimental models (18). C1q-binding amino acid residues underlie IgG–C1q interaction, which forms an initiation complex in the classical complement pathway (22), such as in humoral immunity to pathogens. The pathogens recognized by Abs are cleared by phagocytosis, Ab-dependent cell-mediated cytotoxicity (ADCC), and complement-dependent cytotoxicity (CDC) mechanisms. Interaction of the C1q and IgG Fc region is an initial step in CDC reaction to pathogens (23). The constant 2 (C_H2) domain is the crucial region for C1q binding to the IgG Fc region (24, 25). Mapping studies of C1q-binding residues have demonstrated that the three spatially close sites (K322, P329, and P331) constitute the binding epicenter in the human IgG1 C_H2 domain. E318 and K320 have been shown to play a minor role in complement activation by site-directed mutagenesis studies in vitro. Among different species, these residues are relatively well conserved (22, 25–27). However, the precise role of these binding residues has not been determined in the activation of complement cascades in vivo.

*Department of Dermatology, Hokkaido University, Graduate School of Medicine, Sapporo; and [†]Faculty of Medical and Pharmaceutical Sciences, Kumamoto University, Kumamoto, Japan

[1]Q.L. and H.U. contributed equally to this work.

Received for publication February 26, 2010. Accepted for publication October 4, 2010.

This work was supported by the Program for Promotion of Fundamental Studies in Health Sciences of the National Institute of Biomedical Innovation (06-42 to H.S.) and in part by Grants-in-Aid for Scientific Research (A) (21249063 to H.S.) and (C) (20591312 to A.S.) from the Ministry of Education, Culture, Sports, Science, and Technology of Japan.

Address correspondence and reprint requests to Dr. Akihiko Shibaki and Dr. Hiroshi Shimizu, Department of Dermatology, Hokkaido University Graduate School of Medicine, North 15 West 7, Kita-ku, Sapporo, 060-8638, Japan. E-mail addresses: ashibaki@med.hokudai.ac.jp and shimizu@med.hokudai.ac.jp

The online version of this article contains supplemental material.

Abbreviations used in this paper: ADCC, Ab-dependent cell-mediated cytotoxicity; BMZ, basement membrane zone; BP, bullous pemphigoid; C1q, complement 1q; CDC, complement-dependent cytotoxicity; C_H2, constant 2; COL17, type XVII collagen; DB, dilution buffer; DEJ, dermal-epidermal junction; DIF, direct immunofluorescence; Flu, fluorescence; HSC, human serum complement; IIF, indirect immunofluorescence; NC16A, noncollagenous 16A; NHEK, normal human epidermal keratinocyte; PI, propidium iodide; rh, recombinant human; Sf-9, *Spodoptera frugiperda*-9; VH, V region H chain; VL, V region L chain.

www.jimmunol.org/cgi/doi/10.4049/jimmunol.1000667

IgG1 is thought to be the predominant subclass of anti-hCOL17 IgG autoantibodies in sera from BP patients. Clinical studies have shown a preferential detection of hCOL17-specific IgG1 and IgG4 autoantibodies in BP sera, with IgG2 and IgG3 being detected in a minority of patients (5, 7, 28). Eighty-five percent and 46% of BP sera contained IgG1 and IgG4 Abs against hCOL17, respectively (6). The presence of IgG1 autoantibodies has been associated with active BP phenotypes (5, 6), and the autoantibody level has been correlated with the area of skin blistering (29). These clinical findings indicate that IgG1 might be the main pathogenic subclass in BP. However, to our knowledge, there has been no direct in vivo evidence to demonstrate the pathogenic role of the anti-hCOL17 IgG1 autoantibody until now.

To confirm whether BP IgG1 autoantibodies can induce the BP phenotype in vivo and to analyze the importance of various C1q-binding residues in the IgG1 Fc C_H2 domain in BP, we cloned and constructed a recombinant human (rh)IgG1 mAb against hCOL17 NC16A. By site-directed mutagenesis in the C_H2 domain of the IgG1 mAb Fc region, alanine substitutions were introduced at various residue sites that were previously verified as C1q binding sites in vitro. The blister formation triggered by the non-mutated IgG1 mAb was assessed in vivo using our COL17-humanized ($COL17^{m-/-,\ h+}$) mouse model, which expresses hCOL17 but not mouse COL17 at the BMZ (17). In contrast, the IgG1 mAbs that were mutated at the P331 and/or P329 residue(s) failed to elicit blister formation. Our findings indicate that IgG1 Abs, as the predominant IgG subclass, can induce subepidermal blister formation via IgG Fc–C1q interaction in BP.

Materials and Methods

Establishment of the EBV-transformed B cell clones

PBMCs were prepared from seven active nontreated BP patients by density gradient using Ficoll-Paque PLUS (GE Healthcare, Uppsala, Sweden). The diagnosis of BP was made by the typical clinical and histological manifestations as well as by laboratory data including anti-hCOL17 ELISA and indirect immunofluorescence (IIF). The clinical and immunological characteristics of the BP patients are summarized in Supplemental Table I. B cells were isolated by using microbeads conjugated to anti-human CD19 mAb (Miltenyi Biotec, Bergisch Gladbach, Germany), followed by seeding at 15 cells/well in 96 U-bottom microplates (BD Biosciences, San Jose, CA) in complete RPMI 1640 medium containing 2.5 μg/ml ODN2006 (InvivoGen, San Diego, CA) and incubation for 2 wk with irradiated cord mononuclear cells as the feeder layer cells (50,000/well) in the presence of EBV (30% supernatant of B95.8 cells). The culture supernatants were tested for the presence of anti-hCOL17 NC16A Abs by ELISA coated with rhCOL17 NC16A peptide as reported previously (17). The index values of ELISA were defined by the following formula: index = (OD of tested supernatant − OD of negative control)/(OD of positive control − OD of negative control) × 100 (30–32). As a positive control, we used a standard BP serum supplied with the hCOL17 NC16A-ELISA kit (MESACUP BP180 test; Medical and Biological Laboratories, Nagoya, Japan) as reported previously (17, 33). Adjustment of the values relative to the positive control allows comparison of results from different plates, even if performed under different conditions. Positive wells were cloned by limiting dilution in the presence of ODN2006 and irradiated cord mononuclear cells.

Construction of IgG1 expression vector

L chain (κ and λ) and Fd (V region + constant domain 1) fragments were amplified by RT-PCR from monoclonal B cell clones using general primers for the Ab library (Table I), cloned into pCR2.1 vectors (Invitrogen, Carlsbad, CA), and sequenced by ABI 3100 genetic analyzer (Applied Biosystems, Foster, CA). After introducing one cutting site by the restriction endonucleases EcoRV at the 3′ end, the L chain was inserted into the human IgG1 expression vector pAc-κ-Fc or pAc-λ-Fc (Progen, Heidelberg, Germany) at the SacI and EcoRV cutting sites (Supplemental Fig. 1). Then the Fd sequence was inserted into the vector at the XhoI and SpeI cutting sites. The constructed baculovirus vector containing Fd and $V_{\kappa \text{ or } \lambda}$ genes was transfected to *Spodoptera frugiperda*-9 (Sf-9) insect cells using the BaculoGold Transfection Kit (BD Biosciences). Recombinant baculovirus was harvested from the supernatant of Sf-9 cell culture medium TNM-FH (Grace's insect medium, 10% FBS, and penicillin-streptomycin) (Invitrogen) at 4–5 d after the transfection. Secreted rhIgG1 Abs were detected in the supernatant using an hCOL17 NC16A-ELISA kit (MBL, Nagoya, Japan). The whole procedure followed the manufacturers' recommendations.

Production and purification of the rhIgG1 mAb

The recombinant virus inocula, via three rounds of plaque purification, infected Sf-9 cells at a multiplicity of infection of 0.5–10. The cells were grown in SF-900 II SFM (Life Technologies, Carlsbad, CA) serum-free suspension culture using a spinner 1-L flask with a vertical impeller (Corning, Lowell, MA) at 27°C. One week later, supernatant was harvested and clarified by centrifugation and filtered through 0.45 μM filters (Millipore, Bedford, MA). Purification was performed on HiTrap Protein G column (GE Healthcare). The eluted IgG in 1 M glycine-HCl (pH 2.7) was dialyzed in PBS for at least 48 h and then quantified by spectrophotometer (Pharmacia Biotech, Uppsala, Sweden) at 280 nm.

Generation of the mutated IgG1 mAbs

Alanine substitutions were incorporated into the human IgG1 pAc-λ-Fc vector by site-directed mutagenesis using a Quick Change Mutagenesis Kit (Stratagene, La Jolla, CA), according to the manufacturer's instructions. We constructed seven mutants: five single-site ones and two multisite ones. The mutagenic oligonucleotide primers containing target sites are listed in Table I. Primers were purified by PAGE to prevent the primers from experiencing a significant decrease in mutation efficiency. Sequences were verified by ABI 3100 genetic analyzer (Applied Biosystems). The different constructs were expressed in the Sf-9 cells described above. The IgG was directly purified from the filtered serum-free supernatant using 5 ml HiTrap Protein G column (GE Healthcare).

Establishment of hCOL17-293 cells

To establish the hCOL17-293 cell line, FlpIn 293 cells (Invitrogen) were first cotransfected with the constructed plasmid pcDNA5/FRT (Invitrogen) that had been inserted with the hCOL17 gene (a gift from Dr. K. B. Yancey, University of Texas Southwestern Medical Center, Dallas, TX) and pOG44 (Invitrogen) and were then cultured in selective medium (DMEM, 100 μg/ml hygromycin B [Invitrogen], and 10% FBS). Second, the expression levels of hCOL17 were detected by Western blot analysis using BP serum Abs (1:20) as the first Ab. Eventually, the positive clones were maintained in DMEM containing 50 μg/ml hygromycin B and 10% FBS. The procedures were handled according the manufacturers' recommendations.

Epitope mapping of the IgG1 mAb

We synthesized the N terminus half (hNC16A 1–3, aa 490–534) of the hCOL17 NC16A domain as a GST-fusion protein using the expression vector pGEX2-T (Amersham Biosciences, Uppsala, Sweden) and bacteria B12 (Amersham Biosciences), as reported previously (17, 34). Other peptides including hNC16A 1 (aa 490–506), hNC16A 2 (aa 506–520), hNC16A 2.5 (aa 514–532), and hNC16A 3 (aa 520–534) were expressed in the same way and then purified with a GSTrap FF affinity column (GE Healthcare). The purified IgG1 mAb 3.B6 (0.25 μg/ml) was incubated with the 0.5 μg/lane GST-fusion proteins that were transferred to a 0.2-μm nitrocellulose membrane (Bio-Rad, Richmond, CA) for storage at 4°C overnight. Immunoblots were probed with anti-human IgG polyclonal Abs conjugated with HRP (1:1000; DakoCytomation, Glostrup, Denmark). BP serum from patient 3 (1:30) was acted as the positive control.

Competitive-inhibition assay

Competitive-inhibition ELISA was performed in triplicate as described previously (35). Inhibitor solutions (five subpeptides of the hNC16A, full-length hNC16A, and GST protein) were double serially diluted in 0.5% BSA and mixed with equal volumes of the IgG1 mAb 3.B6 (2.5 μg/ml), then incubated at 37°C for 1 h. One hundred microliters of the mixtures was added to the wells coated with hCOL17 NC16A. The remainder of the assay was performed according to standard procedures. OD was measured at 450 nm.

C1q-binding assay

The C1q-binding activity of the mutated IgG1 mAbs was determined by C1q ELISA-binding assay. The mAbs with double serial dilution (starting concentration: 20 μg/ml) in 0.05 M sodium carbonate buffer (pH 9) were coated in a 96-well plate (Nalge Nunc International, Rochester, NY) and left overnight at 4°C. The plates were washed three times with PBS containing 0.05% Tween 20 and blocked for 1 h at room temperature with

ELISA diluent buffer (BD Biosciences), then incubated for 2 h with 100 μl 4 μg/ml human complement component C1q (Sigma-Aldrich, St. Louis, MO) in ELISA diluent buffer. Then, 100 μl of a 1:400 dilution of sheep polyclonal to C1q (HRP) (Abcam, Tokyo, Japan) was added after washing, and incubation was done for 1 h. Plates were washed five times and displayed in tetramethylbenzidine-soluble reagent (ScyTek, Logan, UT) and then stopped by the addition of 50 μl 20% H_2SO_4 (Wako, Osaka, Japan). The OD was determined at 450 nm. To correct for background, the OD at 450 nm was subtracted from the OD at 620 nm. Binding activity was calculated by the following formula: index value = $(OD_{test} - OD_{blank})/(OD_{St.} - OD_{blank})$, where St. is standard human IgG1 (BD Biosciences) and blank is the diluent buffer.

CDC assay

Serum complements from human (Quidel, San Diego, CA) and mouse (Innovative, Novi, MI) were used for cytotoxicity assay. The mAbs (20–0.04 μg/ml) were diluted with dilution buffer (DB) (DMEM [Life Technologies] [pH 7.2], 2 mM glutamine, 0.1% BSA, and 50 μg/ml hygromycin). The hCOL17-293 cells were washed in DB and resuspended at a density of 10^6 cells/ml. In a typical assay, 50 μl of the mAbs, 50 μl diluted complement, and 50 μl cell suspension were added to flat-bottom tissue culture 96-well plates. The mixture was incubated for 2 h at 37°C in 5% CO_2 incubator to facilitate cell lysis. Then, 50 μl Alamar Blue (Invitrogen) diluted in the DB was added to each well and incubated overnight at 37°C in 5% CO_2 incubator. Fluorescence (Flu) value was monitored at 530-nm excitation wavelength and 630-nm emission wavelength using a 96-well Fluorometer (Berthold, Tokyo, Japan). Reduced Flu units exhibit proportionally to the number of viable cells. The activity of the various mutants was examined by plotting the percent CDC activity against the log of working concentration of the mAb. The Flu value of triplicates was used to calculate the percent cytotoxicity: percent CDC activity = $100 \times (1 - [Flu_{no\ complement} - Flu_{test}]/[Flu_{no\ complement} - Flu_{total\ lysis}])$, where $Flu_{total\ lysis}$ reading from positive control well was incubated for an additional 15 min with lysis solution (Roche, Mannheim, Germany).

ADCC assay

The normal PBMCs were fractionated by Ficoll-Paque PLUS gradient and resuspended in assay reaction buffer (RPMI 1640, 10 mM HEPES, 1% FBS, and 100 μg/ml gentamycin). The hCOL17-293 cells were washed and resuspended in the assay reaction buffer. Double-serial-diluted mAb in a 50-μl assay reaction buffer was incubated with 50 μl target cells (hCOL17-293 cells) (10,000 cells/well) for 30 min at 37°C. Then 50 μl effector cells (normal PBMCs) in a cell suspension (100,000 cells/well) was dispensed into the wells, and incubation was continued for 4 h at 37°C. The activity of lactate dehydrogenase was determined by using the Cytotoxicity Detection PLUS (lactate dehydrogenase) Kit (Roche), according to the manufacturer's instructions. The absorbance (450 nm) of triplicates was used to calculate the percent cytotoxicity: percent cytotoxicity = $100 - 100 \times (OD_{test} - OD_{background})/(OD_{total\ lysis} - OD_{background})$, where $OD_{total\ lysis}$ reading from the positive-control well was incubated for an additional 15 min by lysis solution (Roche).

Passive-transfer models

The Abs including the nonmutated, mutated, BP and healthy serum IgGs were individually injected into 1-d neonatal COL17-humanized ($COL17^{m-/-,\ h+}$) mice at a dose of 25–200 μg/g body weight as described previously (17). At 48 h after i.p. injection of the IgG Abs, skin blister formation was assessed by gentle skin friction. Back skin was used for histological examination (Genetic-Lab, Sapporo, Japan) and direct immunofluorescence (DIF) test using FITC-conjugated polyclonal Ab to human IgG (1:100) (DakoCytomation), murine C1q (1:40) (MBL), and murine C3 (1:200) (Abcam).

Immunofluorescence

Immunofluorescence analysis using the nonmutated or mutated IgG1 mAbs was performed on adult $COL17^{m-/-,\ h+}$ mouse tail, neonatal $COL17^{m-/-,\ h+}$ mouse skin, and normal human skin as described previously (17). Flu labeling was performed with FITC-conjugated secondary Abs (1:100) (DakoCytomation), followed by 10 μg/ml propidium iodide (PI) (Sigma-Aldrich) to counterstain the nuclei. The stained samples were observed and photographed under a confocal laser scanning microscope (Olympus Fluoview FV1000; Olympus, Tokyo, Japan).

Ethical considerations

This study was approved by the Institutional Review Board of Hokkaido University (Sapporo, Japan) and fully informed consent from all patients was obtained for use of human material. All animal operations were approved by and performed in accordance with the Institutional Lab Animal Care and Use Committee of Hokkaido University.

Statistics

Data values were shown as means and/or percentages. We determined statistical significance using Student *t* test or Pearson χ^2 test. One-way or two-way ANOVA test was used for comparing the C1q-binding, CDC, and ADCC activities of the nonmutated and mutated mAbs. A p value <0.05 or 0.01 was considered statistically significant. Analysis was carried out using the statistical software SPSS 10.0 (SPSS, Chicago, IL).

Results

Establishment of immortalized B cell clones derived from BP patients

By means of EBV transformation and limiting dilution (36), three immortalized B cell clones (3.B6, 1.F5, and 7.H8) were established from PBMCs of the seven active BP patients (3.B6 from patient 3, 1.F5 from patient 1, and 7.H8 from patient 7). These three clones stably grew and secreted the IgG mAbs against hCOL17 NC16A. ELISA analysis showed that all the supernatants from the three clones (3.B6, 1.F5, and 7.H8) recognized the rhCOL17 NC16A protein (respective index values [mean ± SD]: 82.99 ± 4.32, 40.18 ± 2.53, and 30.79 ± 1.61). The IgG subclasses of the three clones are IgG1, IgG1, and IgG4, respectively, as determined by gene sequencing. IIF analysis using normal human skin revealed that the supernatants of both 3.B6 and 1.F5 showed linear IgG deposition at the BMZ (Fig. 1*A*, 1*B*). In contrast, the supernatant of clone 7.H8 failed to recognize the BMZ (Fig. 1*C*). We then generated rhIgG1 mAbs containing the Fab regions of these three immortalized B cell clones.

Generation of rhIgG1 mAbs against hCOL17 NC16A

To construct rhIgG1 mAbs, we amplified and cloned the cDNA that encodes IgG L and H chain variable domains ($V_{\kappa\ or\ \lambda}$ and Fd) from the immortalized B cell clones by RT-PCR using Ab library general primers (Table I). The 700-bp L/H chain variable genes (VL/VH) of clones 3.B6, 1.F5, and 7.H8 were cloned and ampli-

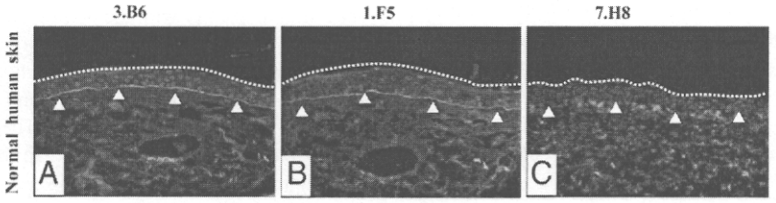

FIGURE 1. Characterization of immortalized B cell clones. IIF analysis was used for detecting the immunoreactivity of the IgG supernatant collected in the first week with normal human skin. Rabbit polyclonal Abs against the H and L chains of human IgG (DakoCytomation) conjugated with FITC were used as secondary Abs (1:100). IgG in the diluted supernatant (1:1) from 2 clones 3.B6 (*A*) and 1.F5 (*B*) deposits linearly (green, FITC) at the DEJ (white arrowheads) (skin surface, white dotted line). Negative staining is observed from clone 7.H8 (*C*). Cell nuclei (red) were counterstained with PI. Original magnification ×200 (*A–C*).

Table I. *General RT-PCR primers for cloning variable genes (V) and the mutagenic primers for substituting alanines at C1q binding sites*

Primers for κ-chain	
HK5	GAMATYGAGCTCACSCAGTCTCCA
HK3	GCGCCGTCTAGAACTAACACTCTCCCCTGTTGAAGCTCTTTGTGACGGGCAAG
Primers for λ-chain	
HL5	CASTYTGAGCTCACKCARCCGCCCTC
HL3	GAGGGATCTAGAATTATGAACATTCTGTAGG
Primers for Fd	
$H_{1,3}$	CAGGTGCAGCTGGTGSAGTCTGG
H_2	CAGGTCAACTTGAAGGAGTCTGG
H_4	CAGGTGCAGCTGCAGGAGTCGGG
V_H5	CAGGTGCAGCTCGAGSAGTCTGG
HG3	GCATGTACTAGTTTTGTCACAAGA
Single-site mutagenic primers	
E318→A	TGGCTGAATGGCAAGGCGTACAAGTGCAAGGTC
K320→A	GCTGAATGGCAAGGAGTACGCGTGCAAGGTCTCCAACAAA
K322→A	GCAAGGAGTACAAGTGCGCGGTCTCCAACAAAGCCC
P329→A	CAACAAAGCCCTCGCAGCCCCCATCGA
P331→A	AGCCCTCCCAGCCGCCATCGAGAAAACC
Multisite mutagenic primers	
E318A K320A K322A	GACTGGCTGAATGGCAAGGCGTACGCGTGCGCGGTCTCCAACAAAGCCCTC
P329A P331A	CAACAAAGCCCTCGCAGCCGCCATCGAGAAAAC

General primers for V_L and Fd chains (M = A, C; Y = C, T; S = G, C; K = G, T; R = A, G). Mutagenic primers at C1q binding sites (only showing the sense primer; the underlined codons are substituted into alanines).

fied by the V_λ/$VH_{1,3}$ V_κ/VH_2, and V_κ/$VH_{1,3}$ subfamily primers, respectively (Table II). Details of the variable gene sequence from the clones are summarized in Supplemental Table II.

Both the VL and VH genes were successively cloned into XhoI/SpeI and SacI/EcoRV sites of the pAc-κ-Fc or pAc-λ-Fc baculovirus IgG1 expression vectors (Supplemental Fig. 1) (37). Recombinant baculovirus was produced by transfecting the recombinant vectors that contained VL/VH genes into Sf-9 insect cells. Postinfection with the purified recombinant baculovirus, the Sf-9 cells secreted rhIgG1 mAbs in the culture supernatant. ELISA analysis showed that the rIgG1 mAb from the clone 3.B6 recognized hCOL17 NC16A (index value [mean ± SD]: 161 ± 5.37) but not the unrelated control protein, human type VII collagen (index value: 2.2 ± 0.04). The human COL17 NC16A ELISA index values of mAbs derived from clones 1.F5 and 7.H8 were 4.23 ± 0.02 and 1.74 ± 0.01, respectively, which are significantly lower than that of clone 3.B6 ($p < 0.01$). This result indicates that the reactivity and/or affinity of IgG Abs secreted from insect cells was altered from those produced by human B cells, possibly as a result of differences in three-dimensional structure, to glycosylation or to other factors, even if the Abs had the same gene sequences as the variable regions (38, 39). For example, N-deglycosylation was even observed to affect the m.w. of the H or L chains of Ch-K20-sf9 (37). IIF analysis demonstrated that the rIgG1 mAb 3.B6 reacted with the BMZ of normal human (Fig. 2*A*) and COL17-humanized ($COL17^{m-/-,\ h+}$) mouse skin (Fig. 2*B*) but not with the wild-type mouse skin (Fig. 2*C*).

The amount of the mAb 3.B6 in the supernatant of the infected Sf-9 cells ranged from 5 to16 μg/ml, values that were determined by sandwich ELISA using sheep anti-human Fab Abs. Kinetic analysis using the Biacore system demonstrated that the mAb 3.B6 had high affinity for $K_D = 5.3 \times 10^{-9}$ M ($K_d = 1.9 \times 10^{-4}$ 1/s; $K_a = 3.6 \times 10^4$ 1/Ms; $K_D = K_d/K_a$). The purified mAb 3.B6 stained the cell surface of the normal human epidermal keratinocytes (Fig. 2*D*) and 293 cells that had been transfected with the hCOL17 gene (Fig. 2*E*), suggesting that this mAb recognizes the extracellular domain of hCOL17.

Table II. *Usage of Ab general primers for cloning variable genes from the B-cell clones*

B Cell Clone	L Chain	VL Subfamily	H Chain	VH Subfamily
3.B6	V_λ	VL1-JL3b	$VH_{1,3}$	VH1-D4-JH6
1.F5	V_κ	VK1-JK3	VH_2	VH2-D6-JH4
7.H8	V_κ	VK1-JK2	$VH_{1,3}$	VH3-D5-JH6

Epitope mapping by Western blot analysis using the rNC16A subpeptides revealed that the mAb 3.B6 specifically reacted with the full-length hNC16A, hNC16A 1–3, hNC16A 2, and hNC16A 2.5 (Fig. 3*A*, 3*B*). Binding inhibition assays demonstrated that two peptides (hNC16A 2 and hNC16A 2.5) sharing seven amino acids inhibited the binding of mAb 3.B6 to the hNC16A in a dose-dependent manner (Fig. 3*C*). Thus, the mAb 3.B6 specifically recognized an epitope present at subregion 2 of the hNC16A domain, which was also recognized by the serum derived from the same donor (patient 3) (Fig. 3*B*).

Generation of rhIgG1 mAbs with mutations at C1q binding sites and characterization of C1q-binding activity

After the binding activity of the IgG1 mAb 3.B6 was verified, site-directed mutagenesis was introduced at the C1q binding sites in the C_H2 domain of the rhIgG1 Fc region. Five independent residues (E318, K320, K322, P329, and P331) were substituted with alanine by single-site or multisite (E318 K320 K322 or P329 P331) mutation in the C_H2 domain. Both IIF and Western blot analysis demonstrated that all the mutated mAbs reacted to the hCOL17 NC16A as specifically as the nonmutated mAb did (data not shown). Kinetic analysis also demonstrated that the mutated mAbs had similar affinity with the nonmutated IgG1 mAb 3.B6 (data not shown).

In contrast, all the mutated mAbs demonstrated significantly reduced binding ability to C1q compared with that of the nonmutated mAb ($p < 0.01$) (Fig. 4). The binding abilities of E318A and K320A were slightly lower than that of the nonmutated mAb. No significant difference was observed between the two mutated mAbs ($p > 0.05$). The K322A, E318A K320A K322A, and P329A mAbs showed half the binding ability of the nonmutated mAb. There were no significant differences among these three mAbs ($p > 0.05$). Alanine substitution at position P331 or P329 P331 seemed to demonstrate the lowest C1q-binding capacity of

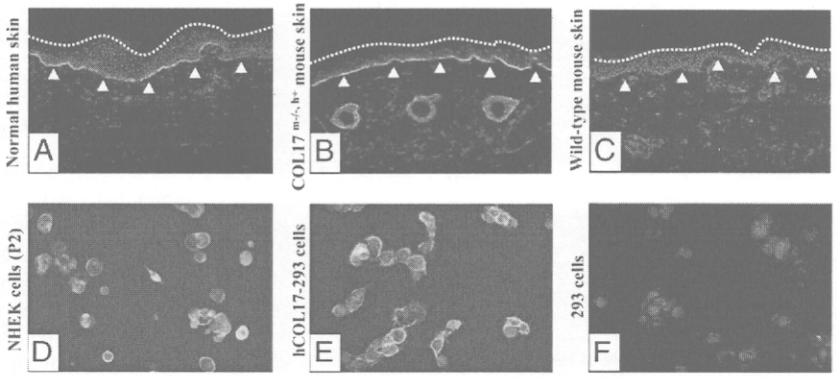

FIGURE 2. Characterization of rhIgG1 mAb 3.B6. Analysis on the specificity of mAb by IIF assay shows that the mAb (green, FITC) deposits linearly at the DEJ (white arrowheads) (skin surface, white dotted line) of normal human (*A*) and COL17-humanized ($COL17^{m-/-,h+}$) mouse skin (*B*), but does not deposit in the wild-type mouse skin (*C*). At the cellular level, the mAb binds to the plasma membrane (green) of second-passage normal human epidermal keratinocytes (NHEKs, P2) (*D*) and hCOL17-293 cells (*E*), but does not bind to 293 cells (negative control) (*F*). Red shows nuclear staining by PI. Original magnification ×100 (*A–C*); ×400 (*E*, *F*).

any of the mutated mAbs. These data indicate that P331 is the most important residue for IgG1 Fc–C1q interaction, followed by the P329, K322, K320, and E318 binding sites in the C1q-binding motif of the Fc C_H2 domain.

In vitro characterization of the CDC and ADCC activities of the mutated IgG1 mAbs

To test the ability of the mutated IgG1 mAbs to activate complement cascade in vitro, CDC assay was carried out using the hCOL17-293 cells as target cells. At 1:20 dilution of human serum complement (HSC), the nonmutated mAb showed the highest CDC activity (Fig. 5*A*). The CDC activity of the two mutated mAbs (E318A and K320A) was nearly half that of the nonmutated mAb, followed in decreasing order by K322A, E318A K320A K322A, and P329A. Their CDC activity was about one-third that of the nonmutated mAb. The mutants P331A and P329A P331A showed very low CDC activity. When the HSC concentration was increased, the percentage of CDC activity increased in the mutants E318A, K320A, K322A, P329A, and E318A K320A K322A (Fig. 5*B*, 5*C*). In contrast, no obvious change was observed in the CDC activity for P331A or P329A P331A, even at the highest HSC concentration (Fig. 5*C*). Similar results were shown when mouse serum complement was used instead of HSC (Fig. 5*D–F*). Taken together, these results indicate that all five residues of the IgG1 C_H2 domain play at least moderate roles and that P331 is the most important residue for activating complements in vitro.

To further investigate whether these mutations affect the Fc-FcγR–mediated ADCC activity of the IgG1 mAbs, we analyzed the mutated mAbs for ADCC activity using the hCOL17-293 cells as target cells and normal PBMCs as effector cells. The mutated mAbs (E318A, K320A, K322A, and E318A K320A K322A) exhibited ADCC activity similar to that of the nonmutated mAb

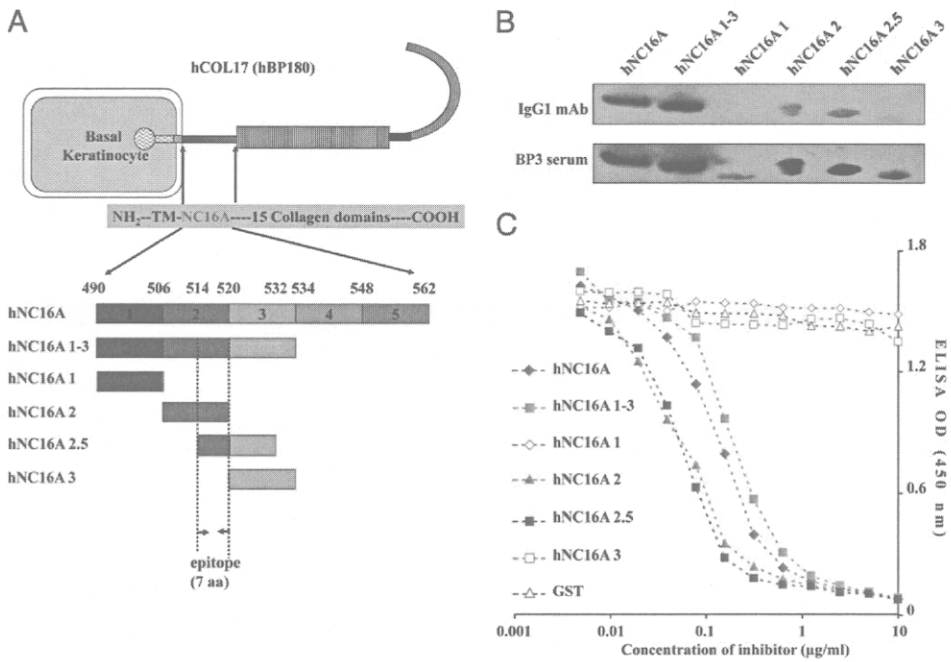

FIGURE 3. Epitope mapping of the IgG1 mAb 3.B6. A schematic map of hCOL17 (hBP180) showing the location of the hNC16A domain and the subpeptides synthesized for epitope mapping studies (*A*). Western blot analysis reveals that the IgG1 mAb recognizes the following subpeptides: hNC16A full-length (aa 490–562), hNC16A 1–3 (aa 490–534), hNC16A 2 (aa 506–520), and hNC16A 2.5 (aa 514–532) (*B*). Two subpeptides (hNC16A 1 and 3) other than the abovementioned four are also recognized by the BP serum from the same donor (patient 3). In ELISA inhibition assay (*C*), the IgG1 mAb 3.B6 (2.5 μg/ml) was incubated with the five subpeptides as inhibitor (10–0.005 μg/ml), with GST protein acting as negative control and hNC16A acting as positive control. The index value of the binding of mAb 3.B6 to the full-length hNC16A was detected by ELISA at OD 450 nm. The three subpeptides (hNC16A 1–3, hNC16A 2, and hNC16A 2.5) almost completely inhibited the binding activity of the IgG1 mAb 3.B6 in a dose-dependent manner. No significant difference in mean inhibitory activity was observed among the three subpeptides ($p > 0.05$ by two-way ANOVA test).

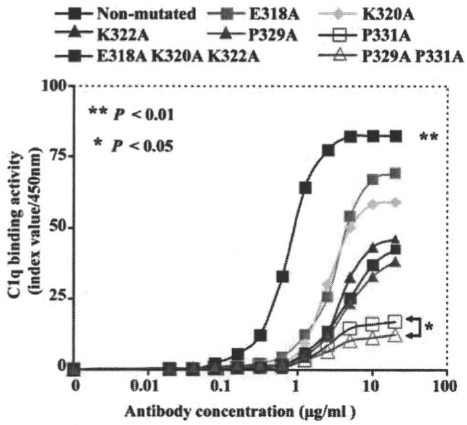

FIGURE 4. C1q-binding activity of the mutated IgG1 mAbs. The ELISA Index value of C1q binding increases gradually with increases in the IgG1 Ab. Maximal binding activity in descending order is nonmutated, then E318A, K320A, K322A, E318A K320A K322A, P329A, P331A and P329A P331A mutated mAbs. Mean index value is higher for the nonmutated mAb than for any other mutated mAbs ($p < 0.01$ by two-way ANOVA test). There is no significant difference in mean index value for E318A versus K320A or for K322 versus E318A K320A K322A or P329A ($p > 0.05$ by one-way ANOVA test). Significant difference is seen between P331A and P329A P331A ($p < 0.05$ by one-way ANOVA test).

(Fig. 6). In contrast, the substitutions at P329 or P329 P331 almost completely eliminated the ADCC activity of the mAbs ($p < 0.01$). Alanine substitution at the P331 site partially decreased the ADCC activity ($p < 0.05$). Altogether, these results suggest that P329 is a critical residue for IgG1–FcγR interaction in vitro.

In vivo functional characterization of the nonmutated and mutated IgG1 mAbs using a COL17-humanized (COL17$^{m-/-,\ h+}$) BP mouse model

To investigate the pathogenic activity of the nonmutated and mutated IgG1 mAbs in vivo, we performed a passive-transfer experiment using neonatal COL17-humanized (*COL17$^{m-/-,\ h+}$*) mice that we had established recently (17). Forty-eight hours after i.p. injection of the nonmutated IgG1 mAb (200 μg/g body weight), eight of nine neonatal mice became erythematous and showed BP-like skin blistering by gentle skin friction (Fig. 7*A*, Table III). Histopathologic examination of the recipient mouse skin confirmed the formation of subepidermal blistering (Fig. 7*B*), infiltration of lymphocytes and neutrophils (Fig. 7*C*), and degranulation of mast cells (Fig. 7*D*). DIF examination revealed the linear deposition of human IgG (Fig. 8*A*) at the BMZ, as well as of mouse C1q (Fig. 8*B*) and C3 (Fig. 8*C*). Administration of the lower dose of the nonmutated IgG1 mAb (100, 50, or 25 μg/g body weight) resulted in a lower frequency of phenotypic changes (five of seven, four of seven, or zero of five mice, respectively) (Table III). ELISA analysis of the sera of recipient mice revealed that the mean index value of the circulating anti-hCOL17 NC16A IgG1 mAbs declined from 55.39 (200 μg/g body weight) to 43.74, 36.91, and 26.53 (100, 50, and 25 μg/g body weight, respectively). Similar results were observed in positive control models with BP patients' IgG autoantibodies (data not shown) in which the BP phenotype was induced as described previously (17).

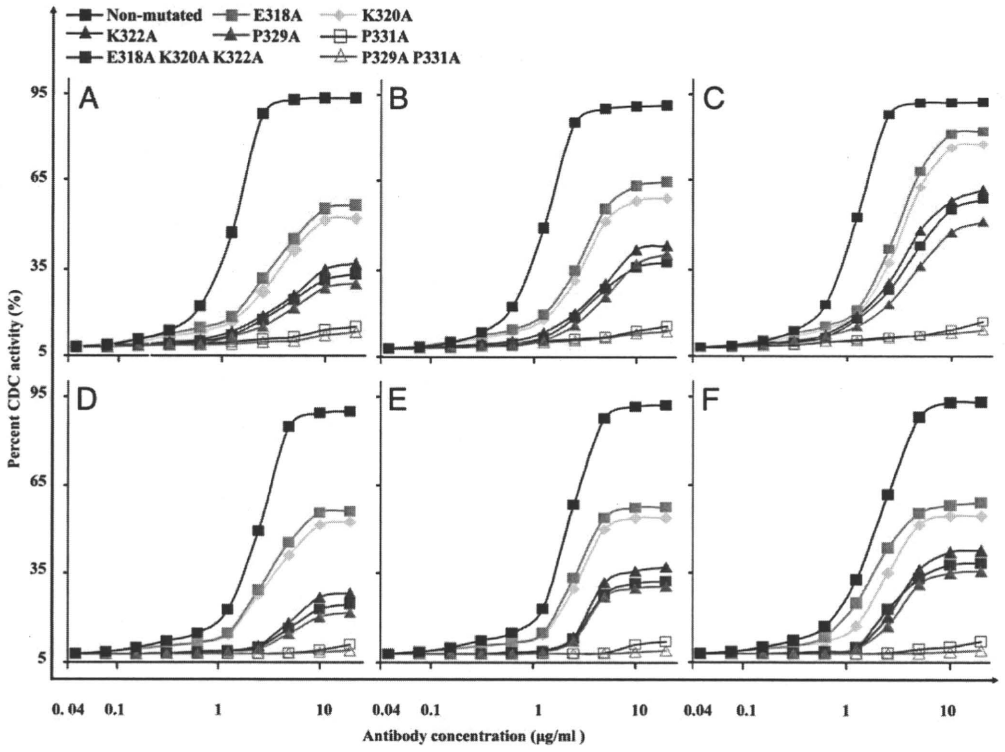

FIGURE 5. Characterization of in vitro CDC activity for the mutated IgG1 mAbs. The nonmutated mAb has the highest percent CDC activity ($p < 0.01$ by one-way ANOVA test) at HSC dilution of 1:20 (*A*), 1:10 (*B*), and 1:5 (*C*), as well as at murine serum complement dilutions of 1:20 (*D*), 1:10 (*E*), and 1:5 (*F*). E318A and K320A have significantly higher CDC activity than K322A, P329A, and E318A K320A K322A ($p < 0.01$ by two-way ANOVA test). No significant difference in the mean percent activity is seen for E318A versus K320A or for K322A versus P329A or versus E318A K320A K322A ($p > 0.05$ by one-way ANOVA test). P331A and P329A P331A show no CDC activity. Significant differences are seen for the two mAbs versus the other mAbs ($p < 0.01$ by two-way ANOVA test).

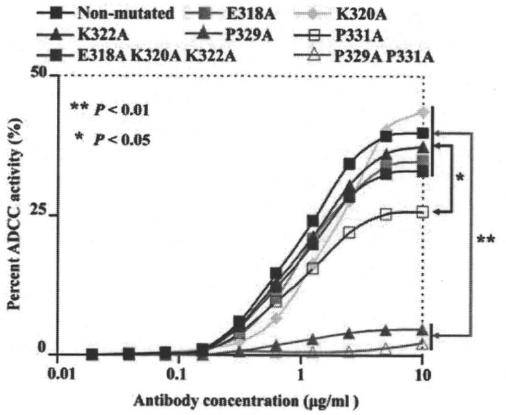

FIGURE 6. Characterization of in vitro ADCC activity for the mutated IgG1 mAbs. In IgG1 mAb-dependent cell-mediated cytotoxicity (ADCC) assay, normal human PBMCs were applied as the effector cells, and hCOL17-293 cells were the target cells. No significant differences in ADCC percent activity are shown for the E318A, K320A, K322A, and E318A K320A K322A versus the nonmutated mAbs ($p > 0.01$ by one-way ANOVA test). ADCC activity is higher for these four mAbs than for P331A ($p < 0.05$ by two-way ANOVA test). The mAbs P329A and P329A P331A show almost no ADCC activity, and significance differences are observed versus the others and nonmutated mAb ($p < 0.01$ by two-way ANOVA test).

In contrast, IgG1 mAbs with the double-site mutation (P329A P331A) completely failed to induce the BP phenotype (zero of eight mice) at the highest dose (200 μg/g body weight), whereas IgG1 mAbs with single-site mutation (P329A or P331A) showed significantly reduced pathogenic capability (one of seven or one of eight mice, respectively) compared with nonmutated IgG1 mAb ($p < 0.01$) (Figs. 7*I–L*, 8*G–I*, Table III). The other three IgG1 mAbs with a single-site mutation (E318A, K320A, or K322A) that showed high or moderate complement activity in vitro elicited skin detachment in the majority of mice at the highest dose (200 μg/g body weight) and demonstrated pathogenic activities in a dose-dependent manner as was true for the non-mutated IgG1 mAb (Figs. 7*E–H*, 8*D–F*). There were no significant differences in positive ratio of skin detachment between these three mAbs and the nonmutated mAb ($p > 0.05$) (Table III). No significant differences were observed in the hCOL17 NC16A-ELISA index values (mean values) of the circulating human IgG Abs in the recipient sera among the mutated or nonmutated IgG1 mAb models at the dose of 200 μg/g body weight ($p > 0.01$).

Discussion

This study provides, to our knowledge, the first direct evidence that human IgG1 Abs against hCOL17 NC16A can induce subepidermal blisters in vivo. BP phenotypic features, including dermal-epidermal separation, deposition of IgG1 Abs C1q and C3, recruitment of neutrophils, and degranulation of mast cells, were successfully reproduced in COL17-humanized ($COL17^{m-/-,\ h+}$) mice by the administration of human IgG1 mAbs against human COL17 NC16A, although the components of the immune system, such as complements and inflammatory cells, are still of murine origin in this experimental model.

It is well known that various IgG subclasses have distinct functional properties. IgG1 and IgG3 are the most effective complement activators, whereas IgG4 is not capable of fixing complements (40). Previous clinical studies demonstrated that IgG1 and IgG4 autoantibodies are major IgG subclasses of BP patient autoantibodies and that IgG2 and IgG3 are minor subclasses of BP patient autoantibodies (5, 7, 28). In vitro analysis using cryosections of human skin and leukocytes from healthy volunteers demonstrated that IgG1 autoantibodies purified from BP sera showed much stronger pathogenic activity than that of IgG4 autoantibodies (41). However, there has been no direct evidence of pathogenic activity of IgG1 autoantibodies in a BP model in vivo. Our group and others have successively reproduced BP phenotypes in COL17-humanized mice by administering IgG autoantibodies prepared from BP patients (15, 17). However, these autoantibodies were poly-

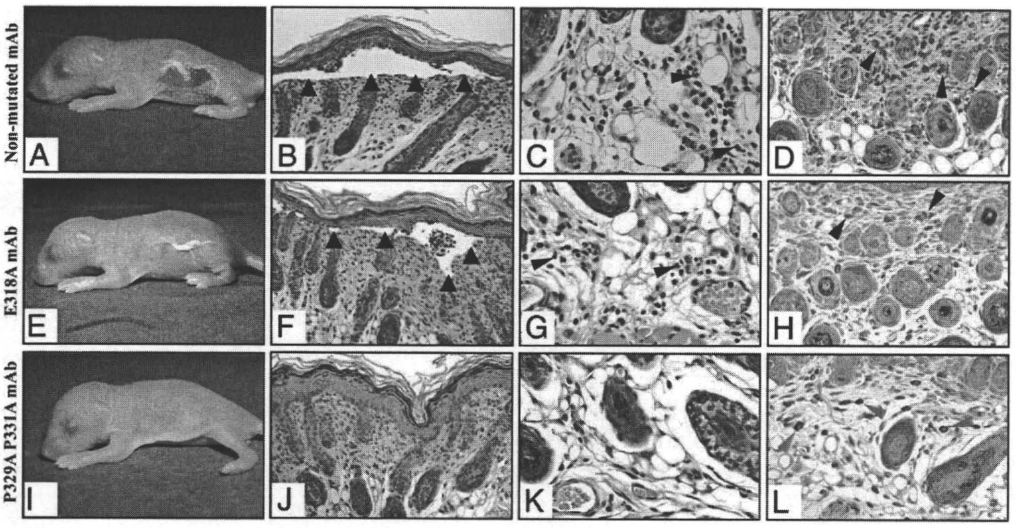

FIGURE 7. Pathogenic activity in vivo of the nonmutated and mutated IgG1 mAbs. The neonatal COL17-humanized ($COL17^{m-/-,\ h+}$) mice were i.p. injected with the nonmutated IgG1 mAb (200 μg/g body weight) or the mutated IgG1 mAbs E318A and P329A P331A (200 μg/g body weight). Forty-eight h later, pathogenic activity was determined by skin blistering test and histology biopsy of back skin including H&E and toluidine blue staining. Skin blistering is positive for the nonmutated and E318A mAbs models (*A*, *E*) and negative for the P329A P331A model (*I*). H&E staining shows epidermal detachment (black arrowheads) at the DEJ in the nonmutated (*B*) and E318A (*F*) mAbs models but not in the P329A P331A model (*J*). The numbers of neutrophils (black arrowheads) and degranulated mast cells (black arrowheads) infiltrating the dermis are more greatly reduced in the P329A P331A (*K*, *L*) model than in the nonmutated (*C*, *D*) and E318A (*G*, *H*) models. Red arrowheads indicate normal undegranulated mast cells. Original magnification ×100 (*B*, *F*, *J*); ×200 (*D*, *H*, *L*); ×400 (*C*, *G*, *K*).

Table III. *Pathogenic activity of the non-mutated and mutated IgG1 mAbs against hCO17 NC16A in the COL17-humanized* ($COL17^{m-/-,h+}$) *BP mouse model*

Abs	Mice with Skin Detachment[a], for Each Injection Dosage (μg/g Body Weight)			
	200 μg	100 μg	50 μg	25 μg
Nonmutated	8/9	5/7	4/7	0/5
Mutated				
E318A	4/6	2/5	0/5	0/4
K322A	5/8	2/6	1/6	1/5
E318A K320A K322A	3/7	2/6	0/5	0/5
P329A	1/7	1/5	0/4	0/5
P331A	1/8	0/7	0/6	0/5
P329A P331A	0/8	0/5	0/4	0/6
Normal human[b]	0/6	—	—	—

[a]Skin blistering test performed at 48 h in neonatal mice.
[b]Human IgG purified from serum in single normal volunteer.

clonal IgG containing all four IgG subclasses. In this study, we have directly demonstrated that anti-hCOL17 NC16A IgG1 mAb has pathogenic activity in vivo by using COL17-humanized ($COL17^{m-/-,h+}$) BP model mice. As previous clinical studies on BP (5, 7, 28), our results further support the notion that IgG1 autoantibodies against hCO17 are potent and possibly the main pathogenic IgG autoantibodies in BP.

Previous studies have demonstrated that activation of the complement pathway is a pivotal step in the BP pathomechanism (17, 18, 42). By comparing nonmutated and/or mutated IgG1 mAbs in terms of pathogenic activity, we have precisely analyzed the roles of C1q-binding residues of the IgG1 Fc region (E318, K320, K322, P329, and P331) in initiating complement activation both in vitro and in vivo. These results are consistent with previous mutagenesis studies that showed that these binding residues are required for complement activation in vitro (22, 25, 27). The alanine substitution at these five single-residue sites variously decreased the CDC activity of the IgG1 mAb against hCOL17 NC16A. The IgG1 mAb that was mutated at P331 showed low CDC activity in vitro, and it failed to produce a BP phenotype in the COL17-humanized ($COL17^{m-/-,h+}$) mice. In contrast, the IgG1 mAbs mutated at K322 or at E318 K320 K322 showed moderate CDC activity in vitro and high (K322) to moderate (E318 K320 K322) pathogenic activity in vivo. The other mutated mAbs (E318A and K320A), which showed high CDC activity in vitro, showed high pathogenic activity in vivo. The results of in vivo pathogenic activity and in vitro CDC and ADCC activities are summarized in Supplemental Table III. The findings suggest that the moderate CDC activity of mutated mAbs is sufficient to induce skin detachment in neonatal COL17-humanized mice and that the P331 residue is the key residue for complement activation and is required for the pathogenic activity of IgG1 mAb in vivo. Thus, complement activation ability seems to correlate with the pathogenic effects of the mutated IgG1 mAbs in COL17-humanized mice (Fig. 5, Table III). Taken together, these findings further suggest that IgG1 Fc-dependent complement activation plays a major pathogenic role in subepidermal blister formation in BP.

In the classical complement pathway, C1q binding to IgG1 triggers proteolytic cascades, which result in the generation of a large amount of C3b. This explains why the immunofluorescence intensity of mouse C1q was weaker than that of mouse C3 in DIF examinations of mouse models, as shown in Fig. 8. In addition to C3b being capable of generating membrane attack complexes as the opsonin, it induces various inflammatory reactions by binding to the complement receptors expressed on the effector cells, such as granulocytes, monocytes, neutrophils, or mast cells (43–45). In our BP mouse model, inflammatory cells, such as mast cells, neutrophils, and lymphocytes, are observed at the dermis. It has been demonstrated that C3 binding to complement receptors stimulates activation and chemotaxis of neutrophils and/or mast cells (46). Mast cells can produce various mediators, such as leukotrienes, platelet-activating factor, and cytokines, that contribute directly or indirectly to neutrophil recruitment (47, 48). The neutrophils recruited into skin then releases elastase and gelatinase B, damaging the BMZ (49, 50). These data suggest that subepidermal blistering is mediated by a complement-dependent cellular (mast-cell and neutrophil) cytotoxicity pathway.

In addition to IgG1 Abs activating complement cascades, they may directly recruit and activate effector cells via the interaction between the Fc region and reciprocal FcγRs. In this study, we analyzed the Fc-FcγR–mediated ADCC activity of IgG1 mAbs. That activity was fully defective in the IgG1 mAb that was mutated at P329, and the mutation at P331 moderately reduced the activity of the IgG1 mAb (Fig. 6). In contrast, the other mutated mAbs (E318A, K320A, K322A, and E318A K320A K322A)

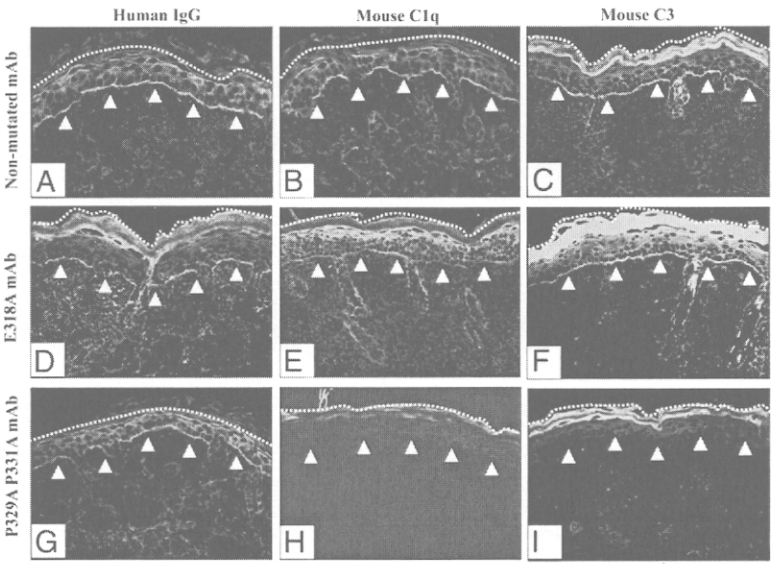

FIGURE 8. Capability of activating complement in vivo for the non-mutated and mutated IgG1 mAbs. In these three models (Fig. 7), 48 h after injection of the IgG1 mAbs, the complement activation capability was determined by DIF of human IgG and mouse complement components C1q and C3. All three of the mAbs (nonmutated IgG1, mutated E318A, and mutated P329A P331A) deposit at the DEJ (white arrowheads) (skin surface, white dotted line) of mouse skin (*A*, *D*, *G*). Mouse complement components C1q and C3 (green, FITC) are activated by the nonmutated (*B*, *C*) and E318A mAbs (*E*, *F*) but not by P329A P331A (*H*, *I*) at the DEJ (white arrowheads). Original magnification ×200 (*A–I*).

showed similar ADCC activity to that of the nonmutated IgG1 mAb. These results indicate that P329 is a key residue in IgG1-dependent ADCC reaction and that P331 plays a minor role in that process. A site-directed mutagenesis study also demonstrated that alanine substitution at the P329 residue causes the dual deficiencies of ADCC and CDC activity in vitro (25). If we focus on the pathogenic activity of IgG1 mAbs in BP, our mutagenesis studies suggest that Fc-FcγR–mediated ADCC activity may have contributed to the blister formation. In this study, in vitro CDC analysis showed that P329A and K322A had similarly moderate CDC activity (Fig. 5) but mutually distinct ADCC activity (Fig. 6). K322A showed normal ADCC activity, and P329A was incapable of triggering the ADCC reaction. Our in vivo results showed almost no skin detachment for the P329A-mutated mAb (one of seven mice) but some skin detachment for the K322A mAb (five of eight mice) (Table III). These results suggest that the ADCC (FcγR-dependent immune reaction) plays a minor but augmenting role in IgG1-dependent blister formation. This concept is further supported by a previous report by Mihai et al. (41) in which the pathogenicity of BP IgG1 and IgG4 autoantibodies was amplified by the additional recruitment of neutrophils and mast cells via Fc–FcγR interaction.

Recently, our group has used a phage display technique to develop a monoclonal Fab Ab against hCOL17 NC16A from BP patients (51). The monoclonal Fab Ab lacked pathogenic activity when administrated to neonatal COL17-humanized ($COL17^{m-/-,\ h+}$) mice. Furthermore, the monoclonal Fab Ab competitively protected the COL17-humanized ($COL17^{m-/-,\ h+}$) mice from the blister formation that would normally be induced by IgG autoantibodies prepared from BP patients. These results are consistent with our current study, and they further suggest the crucial role of the IgG1 Fc region in BP pathomechanism. In addition, complete IgG1 Ab has a longer half-life than Fab Ab in vivo (52, 53). Therefore, our current study raises the possibility that complete IgG1 mAbs with mutation at the C1q binding sites of the Fc region would protect the pathogenic epitopes from attack by the autoantibodies not only in BP but also in other autoimmune diseases in which complement activation plays an essential role.

In conclusion, to our knowledge, this study is the first in vivo evidence that IgG1 Abs targeting hCOL17 NC16A alone can trigger blister formation, and it suggests that IgG1-dependent complement activation via IgG1 Fc–C1q interaction plays a crucial role in BP.

Acknowledgments

We thank Drs. Yasuyuki Fujita, Yasuki Tateishi, and Daichi Hoshina (Hokkaido University Graduate School of Medicine) for kind discussion and technical assistance. We also thank Noriko Ikeda, Yui Kashima, Mika Tanabe, Yuko Hayakawa, and Akari Nagasaki (Hokkaido University Graduate School of Medicine) for technical assistance; Drs. Daisuke Inokuma (Hokkaido University Hospital, Sapporo), Yuka Oguchi, and Kazuo Kodama (JR Sapporo Hospital, Sapporo) for providing BP patient blood; and Dr. Kim B. Yancey for providing hCOL17 cDNA (University of Texas Southwestern Medical Center, Dallas, TX).

Disclosures

The authors have no financial conflicts of interest.

References

1. Gudi, V. S., M. I. White, N. Cruickshank, R. Herriot, S. L. Edwards, F. Nimmo, and A. D. Ormerod. 2005. Annual incidence and mortality of bullous pemphigoid in the Grampian Region of North-east Scotland. *Br. J. Dermatol.* 153: 424–427.
2. Langan, S. M., L. Smeeth, R. Hubbard, K. M. Fleming, C. J. Smith, and J. West. 2008. Bullous pemphigoid and pemphigus vulgaris—incidence and mortality in the UK: population based cohort study. *BMJ* 337: a180.
3. Jordon, R. E., E. H. Beutner, E. Witebsky, G. Blumental, W. L. Hale, and W. F. Lever. 1967. Basement zone antibodies in bullous pemphigoid. *J. Am. Med. Assoc.* 200: 751–756.
4. Nishie, W., D. Sawamura, K. Natsuga, S. Shinkuma, M. Goto, A. Shibaki, H. Ujiie, E. Olasz, K. B. Yancey, and H. Shimizu. 2009. A novel humanized neonatal autoimmune blistering skin disease model induced by maternally transferred antibodies. *J. Immunol.* 183: 4088–4093.
5. Bernard, P., P. Aucouturier, F. Denis, and J. M. Bonnetblanc. 1990. Immunoblot analysis of IgG subclasses of circulating antibodies in bullous pemphigoid. *Clin. Immunol. Immunopathol.* 54: 484–494.
6. Hofmann, S., S. Thoma-Uszynski, T. Hunziker, P. Bernard, C. Koebnick, A. Stauber, G. Schuler, L. Borradori, and M. Hertl. 2002. Severity and phenotype of bullous pemphigoid relate to autoantibody profile against the NH_2- and COOH-terminal regions of the BP180 ectodomain. *J. Invest. Dermatol.* 119: 1065–1073.
7. Laffitte, E., M. Skaria, F. Jaunin, K. Tamm, J. H. Saurat, B. Favre, and L. Borradori. 2001. Autoantibodies to the extracellular and intracellular domain of bullous pemphigoid 180, the putative key autoantigen in bullous pemphigoid, belong predominantly to the IgG1 and IgG4 subclasses. *Br. J. Dermatol.* 144: 760–768.
8. Stanley, J. R., P. Hawley-Nelson, S. H. Yuspa, E. M. Shevach, and S. I. Katz. 1981. Characterization of bullous pemphigoid antigen: a unique basement membrane protein of stratified squamous epithelia. *Cell* 24: 897–903.
9. Sitaru, C., E. Schmidt, S. Petermann, L. S. Munteanu, E. B. Bröcker, and D. Zillikens. 2002. Autoantibodies to bullous pemphigoid antigen 180 induce dermal-epidermal separation in cryosections of human skin. *J. Invest. Dermatol.* 118: 664–671.
10. Giudice, G. J., D. J. Emery, B. D. Zelickson, G. J. Anhalt, Z. Liu, and L. A. Diaz. 1993. Bullous pemphigoid and herpes gestationis autoantibodies recognize a common non-collagenous site on the BP180 ectodomain. *J. Immunol.* 151: 5742–5750.
11. Anhalt, G. J., C. F. Bahn, R. S. Labib, J. J. Voorhees, A. Sugar, and L. A. Diaz. 1981. Pathogenic effects of bullous pemphigoid autoantibodies on rabbit corneal epithelium. *J. Clin. Invest.* 68: 1097–1101.
12. Liu, Z., L. A. Diaz, J. L. Troy, A. F. Taylor, D. J. Emery, J. A. Fairley, and G. J. Giudice. 1993. A passive transfer model of the organ-specific autoimmune disease, bullous pemphigoid, using antibodies generated against the hemidesmosomal antigen, BP180. *J. Clin. Invest.* 92: 2480–2488.
13. Oikarinen, A. I., J. J. Zone, A. R. Ahmed, U. Kiistala, and J. Uitto. 1983. Demonstration of collagenase and elastase activities in the blister fluids from bullous skin diseases: comparison between dermatitis herpetiformis and bullous pemphigoid. *J. Invest. Dermatol.* 81: 261–266.
14. Ståhle-Bäckdahl, M., M. Inoue, G. J. Guidice, and W. C. Parks. 1994. 92-kD Gelatinase is produced by eosinophils at the site of blister formation in bullous pemphigoid and cleaves the extracellular domain of recombinant 180-kD bullous pemphigoid autoantigen. *J. Clin. Invest.* 93: 2022–2030.
15. Liu, Z., W. Sui, M. Zhao, Z. Li, N. Li, R. Thresher, G. J. Giudice, J. A. Fairley, C. Sitaru, D. Zillikens, et al. 2008. Subepidermal blistering induced by human autoantibodies to BP180 requires innate immune players in a humanized bullous pemphigoid mouse model. *J. Autoimmun.* 31: 331–338.
16. Chen, R., G. Ning, M. L. Zhao, M. G. Fleming, L. A. Diaz, Z. Werb, and Z. Liu. 2001. Mast cells play a key role in neutrophil recruitment in experimental bullous pemphigoid. *J. Clin. Invest.* 108: 1151–1158.
17. Nishie, W., D. Sawamura, M. Goto, K. Ito, A. Shibaki, J. R. McMillan, K. Sakai, H. Nakamura, E. Olasz, K. B. Yancey, et al. 2007. Humanization of autoantigen. *Nat. Med.* 13: 378–383.
18. Nelson, K. C., M. Zhao, P. R. Schroeder, N. Li, R. A. Wetsel, L. A. Diaz, and Z. Liu. 2006. Role of different pathways of the complement cascade in experimental bullous pemphigoid. *J. Clin. Invest.* 116: 2892–2900.
19. Jordon, R. E., S. Kawana, and K. A. Fritz. 1985. Immunopathologic mechanisms in pemphigus and bullous pemphigoid. *J. Invest. Dermatol.* 85(Suppl. 1)72s–78s.
20. Provost, T. T., and T. B. Tomasi, Jr. 1973. Evidence for complement activation via the alternate pathway in skin diseases. I. Herpes gestationis, systemic lupus erythematosus, and bullous pemphigoid. *J. Clin. Invest.* 52: 1779–1787.
21. Jordon, R. E., N. K. Day, W. M. Sams, Jr., and R. A. Good. 1973. The complement system in bullous pemphigoid. I. Complement and component levels in sera and blister fluids. *J. Clin. Invest.* 52: 1207–1214.
22. Duncan, A. R., and G. Winter. 1988. The binding site for C1q on IgG. *Nature* 332: 738–740.
23. Burton, D. R. 1985. Immunoglobulin G: functional sites. *Mol. Immunol.* 22: 161–206.
24. Oganesyan, V., C. Gao, L. Shirinian, H. Wu, and W. F. Dall'Acqua. 2008. Structural characterization of a human Fc fragment engineered for lack of effector functions. *Acta Crystallogr. D Biol. Crystallogr.* 64: 700–704.
25. Idusogie, E. E., L. G. Presta, H. Gazzano-Santoro, K. Totpal, P. Y. Wong, M. Ultsch, Y. G. Meng, and M. G. Mulkerrin. 2000. Mapping of the C1q binding site on rituxan, a chimeric antibody with a human IgG1 Fc. *J. Immunol.* 164: 4178–4184.
26. Tao, M. H., R. I. Smith, and S. L. Morrison. 1993. Structural features of human immunoglobulin G that determine isotype-specific differences in complement activation. *J. Exp. Med.* 178: 661–667.
27. Xu, Y., R. Oomen, and M. H. Klein. 1994. Residue at position 331 in the IgG1 and IgG4 C_H2 domains contributes to their differential ability to bind and activate complement. *J. Biol. Chem.* 269: 3469–3474.
28. Döpp, R., E. Schmidt, I. Chimanovitch, M. Leverkus, E. B. Bröcker, and D. Zillikens. 2000. IgG4 and IgE are the major immunoglobulins targeting the

NC16A domain of BP180 in *Bullous pemphigoid*: serum levels of these immunoglobulins reflect disease activity. *J. Am. Acad. Dermatol.* 42: 577–583.
29. Iwata, Y., K. Komura, M. Kodera, T. Usuda, Y. Yokoyama, T. Hara, E. Muroi, F. Ogawa, M. Takenaka, and S. Sato. 2008. Correlation of IgE autoantibody to BP180 with a severe form of bullous pemphigoid. *Arch. Dermatol.* 144: 41–48.
30. Amagai, M., A. Komai, T. Hashimoto, Y. Shirakata, K. Hashimoto, T. Yamada, Y. Kitajima, K. Ohya, H. Iwanami, and T. Nishikawa. 1999. Usefulness of enzyme-linked immunosorbent assay using recombinant desmogleins 1 and 3 for serodiagnosis of pemphigus. *Br. J. Dermatol.* 140: 351–357.
31. Amagai, M., K. Tsunoda, H. Suzuki, K. Nishifuji, S. Koyasu, and T. Nishikawa. 2000. Use of autoantigen-knockout mice in developing an active autoimmune disease model for pemphigus. *J. Clin. Invest.* 105: 625–631.
32. Ujiie, H., A. Shibaki, W. Nishie, D. Sawamura, G. Wang, Y. Tateishi, Q. Li, R. Moriuchi, H. Qiao, H. Nakamura, et al. 2010. A novel active mouse model for bullous pemphigoid targeting humanized pathogenic antigen. *J. Immunol.* 184: 2166–2174.
33. Kobayashi, M., M. Amagai, K. Kuroda-Kinoshita, T. Hashimoto, Y. Shirakata, K. Hashimoto, and T. Nishikawa. 2002. BP180 ELISA using bacterial recombinant NC16a protein as a diagnostic and monitoring tool for bullous pemphigoid. *J. Dermatol. Sci.* 30: 224–232.
34. Zillikens, D., P. A. Rose, S. D. Balding, Z. Liu, M. Olague-Marchan, L. A. Diaz, and G. J. Giudice. 1997. Tight clustering of extracellular BP180 epitopes recognized by bullous pemphigoid autoantibodies. *J. Invest. Dermatol.* 109: 573–579.
35. Galvin, J. E., M. E. Hemric, K. Ward, and M. W. Cunningham. 2000. Cytotoxic mAb from rheumatic carditis recognizes heart valves and laminin. *J. Clin. Invest.* 106: 217–224.
36. Traggiai, E., S. Becker, K. Subbarao, L. Kolesnikova, Y. Uematsu, M. R. Gismondo, B. R. Murphy, R. Rappuoli, and A. Lanzavecchia. 2004. An efficient method to make human monoclonal antibodies from memory B cells: potent neutralization of SARS coronavirus. *Nat. Med.* 10: 871–875.
37. Liang, M., S. Dübel, D. Li, I. Queitsch, W. Li, and E. K. Bautz. 2001. Baculovirus expression cassette vectors for rapid production of complete human IgG from phage display selected antibody fragments. *J. Immunol. Methods* 247: 119–130.
38. Poul, M. A., M. Cerutti, H. Chaabihi, M. Ticchioni, F. X. Deramoudt, A. Bernard, G. Devauchelle, M. Kaczorek, and M. P. Lefranc. 1995. Cassette baculovirus vectors for the production of chimeric, humanized, or human antibodies in insect cells. *Eur. J. Immunol.* 25: 2005–2009.
39. Liang, C. Y., H. Z. Wang, T. X. Li, Z. H. Hu, and X. W. Chen. 2004. High efficiency gene transfer into mammalian kidney cells using baculovirus vectors. *Arch. Virol.* 149: 51–60.
40. Schumaker, V. N., M. A. Calcott, H. L. Spiegelberg, and H. J. Müller-Eberhard. 1976. Ultracentifuge studies of the binding of IgG of different subclasses to the Clq subunit of the first component of complement. *Biochemistry* 15: 5175–5181.
41. Mihai, S., M. T. Chiriac, J. E. Herrero-González, M. Goodall, R. Jefferis, C. O. Savage, D. Zillikens, and C. Sitaru. 2007. IgG4 autoantibodies induce dermal-epidermal separation. *J. Cell. Mol. Med.* 11: 1117–1128.
42. Liu, Z., G. J. Giudice, S. J. Swartz, J. A. Fairley, G. O. Till, J. L. Troy, and L. A. Diaz. 1995. The role of complement in experimental bullous pemphigoid. *J. Clin. Invest.* 95: 1539–1544.
43. Ricklin, D., and J. D. Lambris. 2007. Complement-targeted therapeutics. *Nat. Biotechnol.* 25: 1265–1275.
44. Melamed, J., M. A. Arnaout, and H. R. Colten. 1982. Complement (C3b) interaction with the human granulocyte receptor: correlation of binding of fluid-phase radiolabeled ligand with histaminase release. *J. Immunol.* 128: 2313–2318.
45. Lambris, J. D., D. Ricklin, and B. V. Geisbrecht. 2008. Complement evasion by human pathogens. *Nat. Rev. Microbiol.* 6: 132–142.
46. Müller-Eberhard, H. J. 1988. Molecular organization and function of the complement system. *Annu. Rev. Biochem.* 57: 321–347.
47. Galli, S. J., J. R. Gordon, and B. K. Wershil. 1991. Cytokine production by mast cells and basophils. *Curr. Opin. Immunol.* 3: 865–872.
48. Galli, S. J. 1993. New concepts about the mast cell. *N. Engl. J. Med.* 328: 257–265.
49. Liu, Z., G. J. Giudice, X. Zhou, S. J. Swartz, J. L. Troy, J. A. Fairley, G. O. Till, and L. A. Diaz. 1997. A major role for neutrophils in experimental bullous pemphigoid. *J. Clin. Invest.* 100: 1256–1263.
50. Liu, Z., J. M. Shipley, T. H. Vu, X. Zhou, L. A. Diaz, Z. Werb, and R. M. Senior. 1998. Gelatinase B-deficient mice are resistant to experimental bullous pemphigoid. *J. Exp. Med.* 188: 475–482.
51. Wang, G., H. Ujiie, A. Shibaki, W. Nishie, Y. Tateishi, K. Kikuchi, Q. Li, J. R. McMillan, H. Morioka, D. Sawamura, et al. 2010. Blockade of autoantibody-initiated tissue damage by using recombinant fab antibody fragments against pathogenic autoantigen. *Am. J. Pathol.* 176: 914–925.
52. Holliger, P., and P. J. Hudson. 2005. Engineered antibody fragments and the rise of single domains. *Nat. Biotechnol.* 23: 1126–1136.
53. Kane, S. V., and L. A. Acquah. 2009. Placental transport of immunoglobulins: a clinical review for gastroenterologists who prescribe therapeutic monoclonal antibodies to women during conception and pregnancy. *Am. J. Gastroenterol.* 104: 228–233.

Correspondence

Two cases of cutaneous sporotrichosis in continental/microthermal climate zone: global warming alert?

doi: 10.1111/j.1365-2230.2010.03795.x

Sporotrichosis is commonly encountered in tropical and subtropical areas, but rarely in continental/microthermal climate zones as defined by the Köppen–Geiger Climate Classification.[1] We report two cases of cutaneous sporotrichosis in Hokkaido, an island in the continental/microthermal climate zone in Japan.

Patient 1 was a 55-year-old Japanese woman, who presented in 2009 with a 6-month history of two dark-red, crusted, infiltrated skin lesions measuring about 10 mm and 2 mm, respectively, on the left upper eyelid (Fig. 1a). She was working as a farmer in Hokkaido and had never lived in any other part of Japan. Histopathological examination of haematoxylin and eosin-stained specimens showed a prominent epidermal hyperplasia and abundant inflammatory infiltration in the dermis. Periodic-acid–Schiff (PAS) and Grocott's methenamine silver (GMS) stains revealed a few round and budding yeast-like cells scattered in the dermis, occasionally within a giant cell. Cultures of the tissue sections of lesion on Sabouraud dextrose agar and potato dextrose agar grew dark-brown velvety colonies. Slide cultures from the colonies contained septate branching hyphae, with slender, tapering conidiophores arising at right angles. A sporotrichin skin test gave a positive reaction.

Patient 2 was a 55-year-old man, who presented in 2002 with a chronic erosive nodule measuring 20 × 10 mm on the left mandible, which had been present for over 1 year on 2002 (Fig. 1b). He was working as a carpenter in Hokkaido, and had never lived in any other part of the country. Histopathological analysis found prominent epidermal hyperplasia and a chronic granulomatous inflammatory cell infiltrate. PAS and GMS stained round yeast-like cells scattered throughout the dermis. Cultures of the biopsied tissue samples grown on Sabouraud dextrose agar produced dark-brown velvety colonies. Slide cultures from the colonies contained septate, branching hyphae. Sporotrichin skin test gave a positive reaction.

Cutaneous sporotrichosis is a fungal infection commonly encountered in tropical and subtropical areas.[1] In Japan, > 3500 cases of cutaneous sporotrichosis were reported as of 2001 on Honshu Island, which falls in the temperate/mesothermal climate zone.[2] By contrast, no case reports were reported from Hokkaido in English journals before 2004. Similarly, few cases have been reported in other continental/microthermal climate zone around the world,[3] suggesting that cutaneous sporotrichosis is extremely rare in that zone. This geographical difference in reported cases may be due to the fact that *Sporothrix schenckii*, the pathogenic fungus that causes sporotrichosis, prefers moderate temperatures (around 22 °C).[1] The yearly temperature in Hokkaido

Figure 1 (a) Patient 1. Nodule and papule on the left upper eyelid. (b) Patient 2. Nodule on the left mandible.

averaged for the years 2000–2008 was 9.1 °C, so these results further suggest that *S. schenckii* rarely occurs in Hokkaido. Interestingly, three cases of cutaneous sporotrichosis, including our two, have been reported from Hokkaido in the Japanese literature since 2000, whereas only one case was recorded before 2000. We suggest that the prevalence of cutaneous sporotrichosis in Hokkaido may be increasing as a result of recent global warming.

Acknowledgement

We thank Dr H. I. Shibaki for technical assistance with the cultures.

D. Inokuma, A. Shibaki and H. Shimizu
Department of Dermatology, Hokkaido University Graduate School of Medicine, N15 W7, Sapporo 060-8638, Japan
E-mail: inokuma@med.hokudai.ac.jp
Conflict of interest: none declared.
Accepted for publication 7 December 2009

References

1 Bustamante B, Campos P. Endemic sporotrichosis. *Curr Opin Infect Dis* 2001; **14**: 145–9.
2 Kikuchi I, Morimoto K, Kawana S *et al.* Usefulness of itraconazole for sporotrichosis in Japan: study of three cases and literature comparison of therapeutic effects before and after release on the market. *Eur J Dermatol* 2006; **16**: 42–7.
3 Bargman H. Successful treatment of cutaneous sporotrichosis with liquid nitrogen: report of three cases. *Mycoses* 1995; **38**: 285–7.

The Fas/Fas ligand system, rather than granzyme B, may represent the main mediator of epidermal apoptosis in dermatomyositis

doi: 10.1111/j.1365-2230.2010.03808.x

We read with interest the paper by Grassi *et al.*[1] reporting an immunohistochemical study on cutaneous lesions of lupus erythematosus (CLE) and dermatomyositis (DM). A particularly interesting finding was that the expression of granzyme B (GrB), a pro-apoptotic serine-protease, was higher in CLE rthan in DM lesions. As GrB is mainly expressed by CD8+ lymphocytes, we were puzzled to read that 'in DM, the CD8+ subpopulation represented > 50% of the lymphocytic population'.[1] This finding is in striking contrast to a study in which our research group found that the CD4/CD8 ratio is approximately 2.5 in DM skin lesions.[2] On the other hand, the number of infiltrating CD8+ cells was reported to be similar to that of the CD4+ cells in CLE in both papers.[1,2] As previous studies also reported a similar level of apoptotic phenomena in lesional epidermis in both CLE and DM,[3,4] it is evident that GrB is not likely to represent a major mechanism of cell death in DM lesions.

We report the results from an ongoing study on skin lesions of six patients with DM, five patients with subacute CLE (SCLE) and five patients with discoid CLE (DLE). The sun-protected, clinically healthy skin of the patients served as internal controls, and five healthy donors comprised the control group. Immunohistochemical examination, performed as described previously,[2] included antibodies to Bax, a pro-apoptotic molecule involved in the mitochondrial pathway of apoptosis and activated by GrB; Bcl-2, its antiapoptotic counterpart also belonging to the mitochondrial pathway; Fas and Fas ligand (Fas-L), two key molecules triggering the death receptor pathway of apoptosis; and caspase 3, the final effector of both pathways. The following monoclonal antibodies were used. Bax: 1 : 500 dilution, clone YTH-2D2 (R&D Systems, MN, USA); Bcl-2: 1 : 1000 dilution, clone 124 (Dako, Copenhagen, Denmark); Fas: 1 : 60 dilution, clone GM30 (Novocastra Laboratories Ltd., Newcastle upon Tyne, UK); FasL): 1 : 50 dilution, clone 5D1 (Novocastra); caspase 3: 1 : 50 dilution, clone 5A1 (Cell Signaling, Danvers, MA, USA).

There was higher expression of Bax than of Bcl-2 in patient epidermis (Table 1). Fas was strongly expressed in epidermal sections from patients with DM (Fig. 1a) and CLE, and there was focal positivity in the healthy skin of these patients. Caspase 3 was expressed strongly in all lesional specimens and moderately in the healthy skin of patients.

Table 1 Semiquantitative evaluation of apoptotic molecules in lesional sections and controls.

	DM	DM-HS	SCLE	SCLE-HS	DLE	DLE-HS	HC
Bax	++	++	+++	++	+++	+	+
Bcl-2	+	+	+	+	++	+	+
Fas	+++	+	+++	+	+++	+	−
FasL	++	+	+++	+	++	+	−
Caspase 3	+++	++	+++	++	+++	++	+

DM, lesional epidermis of dermatomyositis; DM-HS, epidermis of sunprotected healthy skin from patients with DM; SCLE, lesional epidermis of subacute cutaneous lupus erythematosus; SCLE-HS, epidermis of sunprotected healthy skin from patients with SCLE; DLE, lesional epidermis of discoid cutaneous lupus erythematosus; DLE-HS, epidermis of sunprotected healthy skin from patients with DLE; HC, epidermis of sunprotected healthy skin from healthy controls. Semiquantitative evaluation of epidermal positivity for Bax, Bcl-2, Fas and caspase 3: −, negative; +, focal; ++, continuous basal; +++, basal and suprabasal. Semiquantitative evaluation of dermal positivity for FasL: −, negative; +, 0–5 cells; ++, 6–10 cells and +++, > 10 cells).

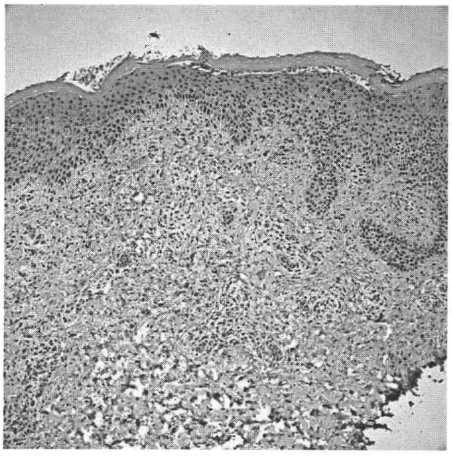

Fig 2. Immunohistochemistry of skin for angiopoietin-2. Note the abundant staining in the basal epidermis and dermal inflammatory cells. (Original magnification: ×100.)

National Institutes of Health, and a Veterans Administration Hospital Merit Award (to J.L.A.)

Conflicts of interest: None declared.

Reprint requests: Jack L. Arbiser, MD, PhD, Department of Dermatology, Emory University School of Medicine, WMB 5309, 1639 Pierce Dr, Atlanta, GA 30322.

E-mail: jarbise@emory.edu

REFERENCES

1. Bhandarkar SS, MacKelfresh J, Fried L, Arbiser JL. Targeted therapy of oral hairy leukoplakia with gentian violet. J Am Acad Dermatol 2008;58:711-2.
2. Lambeth JD, Kawahara T, Diebold B. Regulation of Nox and Duox enzymatic activity and expression. Free Radic Biol Med 2007;43:319-31.
3. Perry BN, Govindarajan B, Bhandarkar SS, Knaus UG, Valo M, Sturk C, et al. Pharmacologic blockade of angiopoietin-2 is efficacious against model hemangiomas in mice. J Invest Dermatol 2006;126:2316-22.
4. Brockow K, Grabenhorst P, Abeck D, Traupe B, Ring J, Hoppe U, et al. Effect of gentian violet, corticosteroid and tar preparations in *Staphylococcus aureus*–colonized atopic eczema. Dermatology 1999;199:231-6.
5. Howell MD, Novak N, Bieber T, Pastore S, Girolomoni G, Boguniewicz M, et al. Interleukin-10 downregulates anti-microbial peptide expression in atopic dermatitis. J Invest Dermatol 2005;125:738-45.

doi:10.1016/j.jaad.2009.05.027

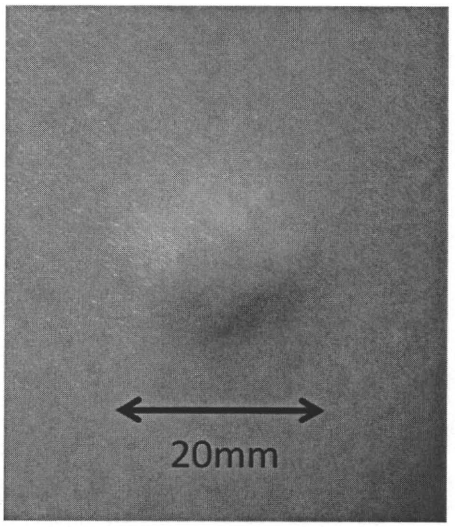

Fig 1. A slightly violaceous nodule on the middle aspect of the left thigh.

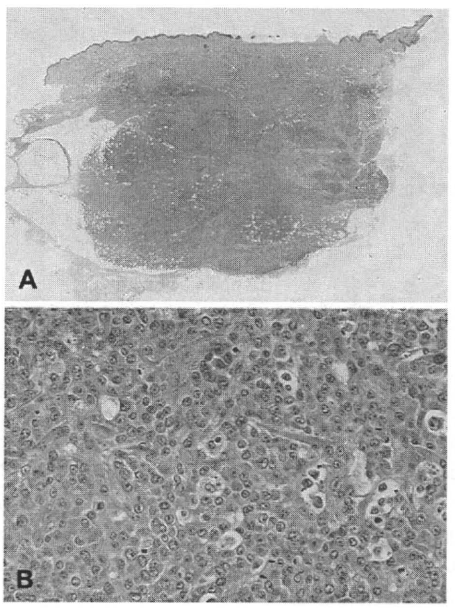

Fig 2. Skin biopsy findings. **A**, Dense, nodular, diffuse infiltrate of monotonous uniform cells involving the dermis and subcutaneous fat. **B**, A nodule of cells with round nuclei; prominent single or multiple nucleoli; abundant pale, slightly eosinophilic cytoplasm; and a number of atypical mitotic figures.

Aleukemic leukemia cutis with extensive bone involvement

To the Editor: Aleukemic leukemia cutis (ALC) is a rare condition that is characterized by the invasion of leukemic cells into the skin before such cells are observed in the peripheral blood.[1] We present a case of ALC with multiple bone metastases.

An 81-year-old man had a 2-month history of asymptomatic nodules on his trunk and legs. The physical examination revealed five subcutaneous nodules measuring up to 10 mm in size on his back and legs and a firm, slightly violaceous nodule

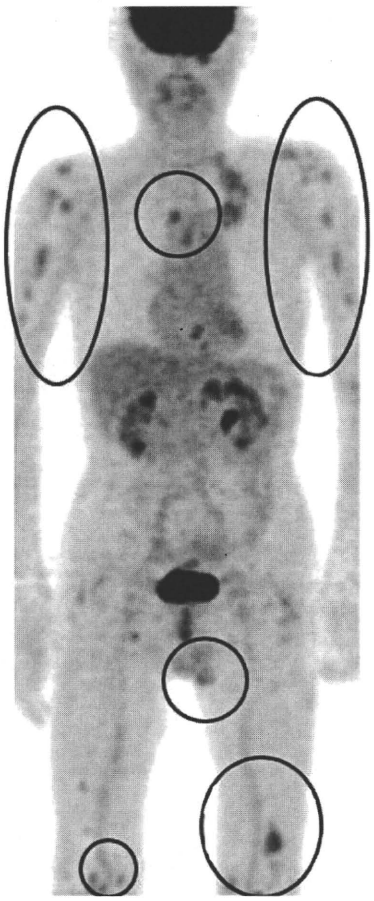

Fig 3. A positron emission tomography scan reveals extensive high-density areas in the bone and in the subcutaneous tissue of the trunk and the extremities, suggesting multiple metastases.

measuring 20 mm in diameter on the middle aspect of his left thigh (Fig 1). A complete blood cell count and chemical analysis showed no pathologic changes. Histopathologic examination of a skin biopsy specimen revealed a dense, nodular, diffuse infiltrate of monotonous uniform cells with round nuclei, prominent single or multiple nucleoli, and abundant pale, slightly eosinophilic cytoplasmic cells throughout the dermis and subcutaneous fat (Fig 2, *A*). A number of atypical mitotic figures were seen (Fig 2, *B*). The tumor cells were positive for leukocyte common antigen, CD68, and myeloperoxidase. A histologic diagnosis of myeloid leukemia cutis with possible monocytic lineage was made. However, bone marrow aspiration showed neither an increase in blasts nor abnormal cell infiltration, and repeated peripheral blood cell counts were normal, with no atypical cells. A diagnosis of ALC was established. Positron emission tomography (PET) revealed extensive high-density areas in the bone and subcutaneous tissue, suggesting multiple metastases (Fig 3). Seven weeks after his first visit, a peripheral blood cell examination disclosed 8% atypical monocytic cells, suggesting a diagnosis of acute myeloid leukemia. The patient refused other studies and died 1 week later.

ALC is a rare form of leukemia with a poor prognosis. The term "aleukemic" has been used to designate a form of leukemia in which there are no leukemic cells in the blood.[2] ALC precedes peripheral blood or bone marrow abnormalities at least 1 month before the systemic findings. Once leukemic cells appear in the peripheral blood or bone marrow, the mean survival time ranges from 3 to 30 months.[3,4] The clinical features of ALC include multiple papules, nodules, or infiltrated plaques with a red-brown or plum-colored surface. Histologic findings show the infiltration of leukemic cells in the dermal or subcutaneous tissues. The cytologic features of the tumor cells include large, vesicular nuclei and multiple prominent nucleoli.[3] Because of the rarity of the disease, there is no consensus on the treatment of choice for ALC; radiotherapy, chemotherapy, and total body electron therapy have achieved variable results.[1,3-8] A study by Chang et al[4] of a large group of ALC patients showed that the most common extramedullary site of involvement after the skin (31 of 31 patients) was the lymph nodes (8 of 31 patients) followed by the spleen (2 of 31 patients). Although no reports of a clinical presentation of ALC with multiple sites of bone infiltration were found in a thorough search of the English-language literature, extramedullary leukemia is known to occur in bone.[5] We emphasize that the routine assessment of a patient with ALC should include systemic investigations such as PET, taking into consideration the possibility of bone involvement.

Maria Maroto Iitani, MD, MSc,[a] Riichiro Abe, MD, PhD,[a] Teruki Yanagi, MD,[a] Asuka Hamasaka, MD, PhD,[a] Yasuki Tateishi, MD, PhD,[a] Yukiko Abe, MD, PhD,[a] Miki Ito, MD,[b] Takeshi Kondo, MD, PhD,[c] Kanako Kubota, MD, PhD,[d] and Hiroshi Shimizu, MD, PhD[a]

Departments of Dermatology, Hokkaido University Graduate School of Medicine[a] and the National Hospital Organization Hokkaido Cancer Center[b]; Departments of Gastroenterology and Hematology,[c] Hokkaido University Graduate School of Medicine; and the Department of Surgical Pathology,[d] Hokkaido University Hospital, Sapporo, Japan

Funding sources: None.

Conflicts of interest: None declared.

Reprint requests: Maria Maroto Iitani, MD, MSc, Department of Dermatology, Hokkaido University Graduate School of Medicine, North 15, West 7, Kita-ku, Sapporo 060-8638, Japan.

E-mail: miitani@med.hokudai.ac.jp

REFERENCES

1. Ohno S, Yokoo T, Ohta M, Yamamoto M, Danno K, Hamato N, et al. Aleukemic leukemia cutis. J Am Acad Dermatol 1990;22 (2 pt 2):374-7.
2. Yoder FW, Shuen RL. Aleukemic leukemia cutis. Arch Dermatol 1976;112:367-9.
3. Okun MM, Fitzgibbon J, Nahass GT, Forsman K. Aleukemic leukemia cutis, myeloid subtype. Eur J Dermatol 1995;5:290-3.
4. Chang H, Shih LY, Kuo TT. Primary aleukemic myeloid leukemia cutis treated successfully with combination chemotherapy: report of a case and review of the literature. Ann Hematol 2003;82:435-9.
5. Lee B, Fatterpekar GM, Kim W, Som PM. Granulocytic sarcoma of the temporal bone. AJNR Am J Neuroradiol 2002;23:1497-9.
6. Török L, Lueff S, Garay G, Tápai M. Monocytic aleukemic leukemia cutis. J Eur Acad Dermatol Venerol 1999;13:54-8.
7. Tomasini C, Quaglino P, Novelli M, Fierro MT. "Aleukemic" granulomatous leukemia cutis. Am J Dermatopathol 1998;20:417-21.
8. Imanaka K, Fujiwara K, Satoh K, Kuroda Y, Takahashi M, Sadatoh N, et al. A case of aleukemic monocytic leukemia cutis treated with total body electron therapy. Radiat Med 1988;6:229-31.

doi:10.1016/j.jaad.2009.05.040

Onychopapilloma presenting as longitudinal leukonychia

To the Editor: Onychopapilloma is an uncommon benign nail neoplasm characterized histologically by distal subungal hyperkeratosis and nail matrix metaplasia of the nail bed with marked papillomatosis. The majority of cases present clinically as localized longitudinal erythronychia. We report a case of onychopapilloma presenting as localized longitudinal leukonychia.

A 50-year-old woman was referred for the evaluation of dystrophy of the right third fingernail. The nail plate had split distally for several years. Her medical history was noncontributory. The physical examination revealed a 1-mm wide band of longitudinal leukonychia with a slight longitudinal ridge on the right third fingernail. No erythronychia was present. Distally, there was a V-shaped notch and split, with a keratotic 1-mm papule at the hyponychium (Fig 1). The other nails were normal. Lateral nail plate curl avulsion exposed a longitudinal ridge extending from the midmatrix onto the nail bed. A longitudinal biopsy from matrix to hyponychium was performed. On histologic examination, the nail bed exhibited slender, elongated, and hyperplastic rete ridges with underlying fibrosis and thickening of the fibrovascular dermal stroma. Upper nail bed keratinocytes were large and exhibited ample pink cytoplasm similar to the nail matrix keratogenous zone. Hyperkeratosis was seen at the hyponychium (Fig 2). A periodic acid–Schiff test did not reveal fungal elements. These findings were consistent with the diagnosis of onychopapilloma.

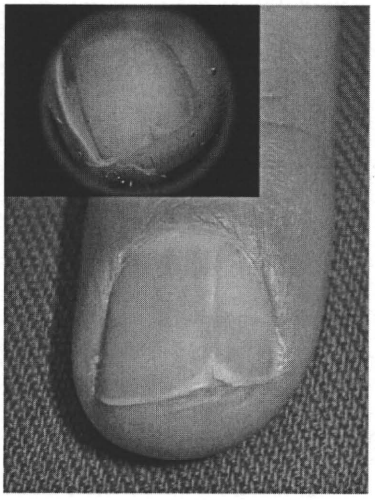

Fig 1. Fingernail with a 1-mm wide band of longitudinal leukonychia and distal V-shaped splitting, onycholysis, and a keratotic papule at the free edge of the nail. Dermatoscopy highlights these findings (*inset*).

Onychopapilloma was first reported in 1995 by Baran and Perrin,[1] who described four cases of "distal subungual keratosis with multinucleate cells." The term "onychopapilloma" was later coined in 2000 when the authors reported a second series of 14 cases with similar clinical and histopathologic features.[2] Key among these features were the upper cell layers in the nail bed epithelium exhibiting abundant eosinophilic cytoplasm resembling the nail matrix keratogenous zone, and was thought to indicate matrix metaplasia of the nail bed epithelium. Additional findings included acanthosis and papillomatosis of the distal nail bed epithelium. Multinucleated cells were found variably. In both series, all lesions presented as either longitudinal erythronychia or longitudinal bands of splinter hemorrhages, several of which were associated with distal onycholysis. Other occurrences of suspected onychopapilloma have been reported, including one case representing solitary nail bed lichen planus, and also in the spectrum of localized longitudinal erythronychia.[3] In addition to onychopapilloma, the differential diagnosis for localized longitudinal erythronychia includes Bowen disease,[2,3] and histologic investigation is often warranted.

Squamous Cell Carcinoma in a Chronic Genital Ulcer in Behçet's Disease

Hiroo Hata, Satoru Aoyagi, Maria Maroto Iitani, Erina Homma and Hiroshi Shimizu
Department of Dermatology, Hokkaido University Graduate School of Medicine, Kita-ku, Sapporo 060-8638, Japan. E-mail: hata07@med.hokudai.ac.jp
Accepted March 30, 2010.

Behçet's disease (BD) is a chronic inflammatory disease characterized by oral aphthae, genital ulcers, non-bacterial folliculitis, erythema nodosum and uveitis. The genital ulcers are characterized by clear demarcation, great depth and pain. They heal and recur, leaving scarring. In a chronic BD ulcer, squamous cell carcinoma (SCC) may develop at the scar site, as is the case with other chronic ulcers that are predisposed to malignancy. However, no cases have been reported in which SCC *in situ* has developed on a chronic genital ulcer in a patient with BD. We describe such a case here.

CASE REPORT

A 74-year-old woman presented with a 2-year history of erosive plaques in the genital region. The lesions had gradually enlarged during the previous 6 months. She had a 20-year history of repeated oral aphthae, genital ulcers and erythema nodosum. BD had been diagnosed 20 years previously. Oral corticosteroids (10 mg/day) had been administered since the initial diagnosis. Furthermore, 6 years prior to presentation, SCC had been observed on her buccal mucosa, for which she had received radiation therapy. No local recurrence had been observed.

Upon physical examination, pale-red, well-demarcated, flatly elevated lesions were extensively found symmetrically on the labia majora. The lesions were partially papillomatous and erosive (Fig. 1). Clinically, the vaginal and urethral mucosa showed no evidence of tumour spreading.

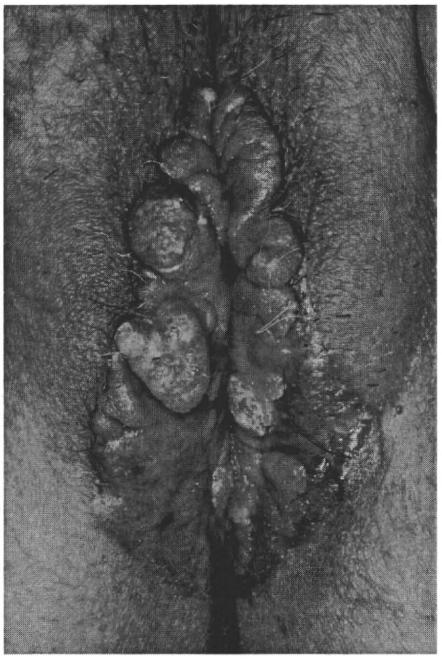

Fig. 1. Clinical features of the tumour. Well-demarcated, slightly reddish, partly papillomatous tumour presents, mainly on the labia majora.

A punch biopsy from the large plaque on the right labium majus showed proliferation of atypical keratinocytes within the acanthotic epidermis; however, the epidermal basement membrane was unaffected.

Routine laboratory examinations including that of serum SCC antigen were normal. Additionally, a computed tomography scan showed no evident distant metastasis, including of the regional lymph nodes. Therefore, the lesion was excised with at least a 1-cm margin. The surgical specimen showed neoplastic proliferation of squamous differentiated tumour cells with dyskeratotic and atypical keratinocytes (Fig. 2a). There was no evidence of dermal invasion by tumour cells (Fig. 2b). The tumour cells tested negative for anti-human papillomatous virus (HPV) antibody by immunostaining; furthermore, HPV DNA was not detected by PCR. We diagnosed this case as SCC *in situ*. The patient was disease-free 6 months after surgery with no recurrence or metastasis.

DISCUSSION

It is extremely rare for a cutaneous neoplasm to develop in cases of BD (1). To the best of our knowledge, only one such case has been reported, in which a patient with BD subsequently developed a Merkel cell carcinoma on the left forearm (2). The authors of that report suggested that immunosuppression due to the treatment for BD might have triggered the Merkel cell carcinoma, although the occurrence of BD with solid tumours tends to be regarded as coincidental.

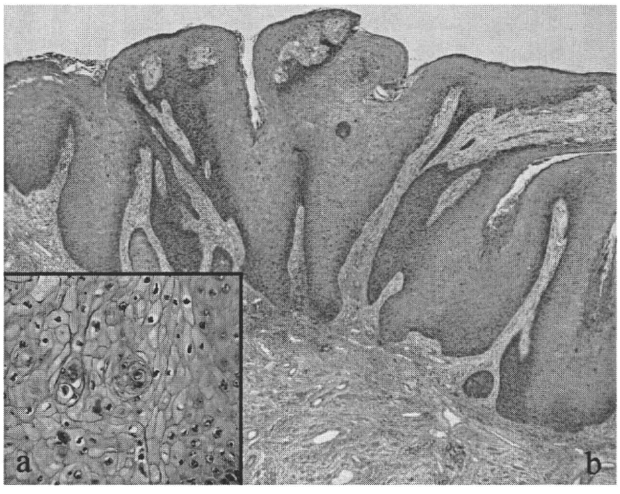

Fig. 2. (a) Neoplastic proliferation of squamous differentiated tumour cells with dyskeratotic and atypical keratinocytes only in the epidermis. These typical keratinocytes and mitoses are scattered throughout the all layers (haematoxylin and eosin; H&E). (b) There is no evidence of dermal invasion by tumour cells (H&E).

Conditions known to be associated with increased risk of SCC *in situ* include therapeutic immunosuppression, arsenic exposure, irradiation, burn scarring, and HPV infection. In addition, HPV infection has been identified in erythroplasia of Queyrat, an intraepidermal carcinoma of the penis (3).

In our case, the refractory genital ulcer and long-term administration of oral corticosteroids may have contributed to the development of the SCC. Interestingly, our case also had a history of SCC on the buccal mucosa. The incidence of SCC *in situ* in patients with BD may be rarer than that in lichen planus or lichen sclerosis et atrophicus patients, given that similar cases have not been reported in patients with BD.

REFERENCES

1. Mansur AT, Kocaayan N, Serdar ZA, Alptekin F. Giant oral ulcers of Behçet's disease mimicking squamous cell carcinoma. Acta Derm Venereol 2005; 85: 532–534.
2. Satolli F, Venturi C, Vescovi V, Morrone P, Panfilis GD. Merkel-cell carcinoma in Behçet's disease. Acta Derm Venereol 2005; 85: 79.
3. Arlette JP. Treatment of Bowen's disease and erythroplasia of Queyrat. Br J Dermatol 2003; 149: 43–47.

severe chronic upper airway disease (SCUAD). J Allergy Clin Immunol 2009;124: 428-33.
4. Okano M, Fujiwara T, Haruna T, Kariya S, Makihara S, Higaki T, et al. PGE_2 suppresses staphylococcal enterotoxin-induced eosinophilia-associated cellular responses dominantly via an EP2-mediated pathway in nasal polyps. J Allergy Clin Immunol 2009;123:868-74.
5. Bachert C, Zhang N, van Zele T, Gevaert P, Patou J, van Cauwenberge P. *Staphylococcus aureus* enterotoxins as immune stimulants. In: Halilos DL, Baroody FM, editors. Chronic rhinosinusitis. Pathogenesis and medical management. New York: Informa Healthcare USA; 2007. p. 163-75.
6. Napolitani G, Acosta-Rodriguez EV, Lanzavecchia A, Sallusto F. Prostaglandin E_2 enhances Th17 responses via modulation of IL-17 and IFN-γ production by human CD4+ T cells. Eur J Immunol 2009;39:1-12.
7. Saito T, Kusunoki T, Yao T, Kawano K, Kojima Y, Miyahara K, et al. Role of interleukin-17A in the eosinophil accumulation and mucosal remodeling in chronic rhinosinusitis with nasal polyps associated with asthma. Int Arch Allergy Immunol 2009;151:8-16.
8. Su YC, Rolph MS, Hansbro NG, Mackay CR, Sewell WA. Granulocyte-macrophage colony-stimulating factor is required for bronchial eosinophilia in a murine model of allergic airway inflammation. J Immunol 2008;180:2600-7.
9. Doganci A, Eigenbrod T, Krug N, De Sanctis GT, Hausding M, Erpenbeck VJ, et al. The IL-6R alpha chain controls lung CD4+CD25+ Treg development and function during allergic airway inflammation in vivo. J Clin Invest 2005; 115:313-25.

Available online July 12, 2010.
doi:10.1016/j.jaci.2010.05.014

Topical application of dehydroxymethylepoxyquinomicin improves allergic inflammation via NF-κB inhibition

To the Editor:

Atopic dermatitis (AD) is a chronic, relapsing inflammatory skin disease with significant morbidity and an adverse impact on patient well-being. AD has become increasingly prevalent in industrialized countries, where it now occurs in 10% to 20% of children and 1% to 3% adults.[1] Corticosteroids are generally prescribed to control the symptoms, yet repeated use can cause severe skin atrophy and susceptibility to infection.[2] Tacrolimus, a calcineurin inhibitor, has recently gained widespread use as an AD treatment that avoids the typical side effects associated with topical corticosteroids.[3] However, refractory AD can remain even in patients treated with both corticosteroid and tacrolimus.

Dehydroxymethylepoxyquinomicin (DHMEQ), a newly developed low-molecular-weight nuclear factor- κB (NF-κB) inhibitor, is a 5-dehydroxymethyl derivative of the antibiotic epoxyquinomicin C.[4] DHMEQ has been found to inhibit TNF-α–induced NF-κB activation by suppressing nuclear translocation but not IκB phosphorylation or degradation.[5] Recently the antitumor effects of DHMEQ on breast,[6] thyroid,[7] and prostate[8] cancers as well as its anti-inflammatory and immunosuppressive effects have been reported in mice models.[9,10] In this study, we used atopic dermatitis model mice to examine the antiallergic inflammation efficacy of DHMEQ.

We confirmed that DHMEQ effectively inhibited the NF-κB activity in macrophage-like cell line, RAW264.7 with LPS stimulation (Fig 1, *A*).

First we examined whether DHMEQ suppressed contact hypersensitivity response. Balb/c mice were sensitized with 2,4,6-trinitrochlorobenzene (TNCB) to the dorsal skin and challenged 5 days later on the dorsal surface of the right ear. Immediately after the challenge, DHMEQ (1 mg/mL in acetone) or tacrolimus ointment (1%) was applied to the same ear. The DHMEQ-treated ears showed significantly less ear swelling than the tacrolimus-treated ears (Fig 1, *B*). The suppressive effect of DHMEQ was dose-dependent (Fig 1, *C*). Furthermore, expression of inflammatory cytokine mRNA (IL-1β, IL-6, TNF-α) in lesional skin was suppressed by DHMEQ ointment as well as by tacrolimus ointment (Fig 1, *D*). These data show that DHMEQ suppresses inflammation via suppression of inflammatory cytokine expression regulated by NF-κB.

We next examined whether DHMEQ would inhibit hapten-induced Langerhans cell (LC) migration. Treatment with TNCB caused a significant decline in epidermal LC density 4 hours after application in the untreated mice (30.5%). In contrast, TNCB treatment failed to provoke a significant epidermal LC migration response in the DHMEQ-treated mice (13.1%; Fig 1, *E*). We further evaluated LC morphology in the epidermal sheet preparations derived from the untreated and DHMEQ-treated mice. As illustrated in Fig 1, *F (left)*, at 4 hours after exposure to TNCB, the LCs in the control mice appeared to be activated and to have extended dendritic processes, whereas no such morphologic changes were evident in the LCs examined in the DHMEQ-treated mice (Fig 1, *F, right*). These data support that the DHMEQ suppressed the contact hypersensitivity response at least in part by inhibition of LC migration.

To determine whether DHMEQ has any therapeutic effect in AD, we applied DHMEQ to AD-like lesions of NC/Nga mice and evaluated the progression of skin changes. NC/Nga mice were the spontaneous mouse models of AD. Another spontaneous mouse model, the DS-Nh mouse, has a mutation of transient receptor potential vanilloid 3,[11] whereas the genetic defect of NC/Nga is not known. We used conventional NC/Nga mice that presented severe skin lesions very similar to those of human AD.[12] Conventional NC/Nga mice with moderate to severe AD were topically applied with 1% DHEMQ in plastibase (5% polyethylene and 95% mineral oil), 0.1% tacrolimus ointment, or 0.12% betamethasone ointment daily for 2 weeks. The clinical severity of skin lesion was scored daily according to the 5 main clinical symptoms: scratch behavior, erythema/hemorrhaging, edema, excoriation/erosion, and scaling/dryness.[12] Topical DHMEQ application significantly improved the severity of skin lesions compared with the ointment base as well compared with topical treatment with the 0.1% tacrolimus or 0.12% betamethasone ointment (Fig 2, *A and B*). Improvement of clinical skin condition by DHMEQ was also confirmed by histologic observation, which showed amelioration of hyperkeratosis, acanthosis, dermal edema, and infiltration of the inflammatory cells compared with the ointment base treatment (Fig 2, *C*). At the affected skin sites, the numbers of eosinophils and mast cells were significantly lower in the DHMEQ-treated mice than those in the control mice (Fig 2, *C*).

Potential side effects of topical application of NF-κB inhibition might include susceptibility to infection via local immune suppression. However NF-κB inhibitor presumably avoids the typical side effects associated with topical corticosteroids as well as tacrolimus.

Several reagents targeting NF-κB have been reported. For example, NF-κB decoy oligodeoxynucleotides were reported to be effective in resolving atopic skin lesions in NC/Nga mice.[13] IMD-0354, a selective IKK inhibitor, also improved AD manifestation in model mice.[14] In contrast with these, DHMEQ inhibits NF-κB activation by suppressing nuclear translocation but not IκB phosphorylation or degradation.[5] Because DHMEQ has a unique mechanism to inhibit NF-κB activation, DHMEQ might be effective for AD that does not respond to tacrolimus or corticosteroid, and it might have additive effects with other reagents.